5. Results

5.1. Unilateral and bilateral renal ischemia-reperfusion injury model standardization

Initially, DM and ND rats have performed bilateral ischemia by clamping both renal pedicles for 60 min followed by 1 week of reperfusion. And, we recorded animal death after renal ischemia ***(Figure 5.1)***.

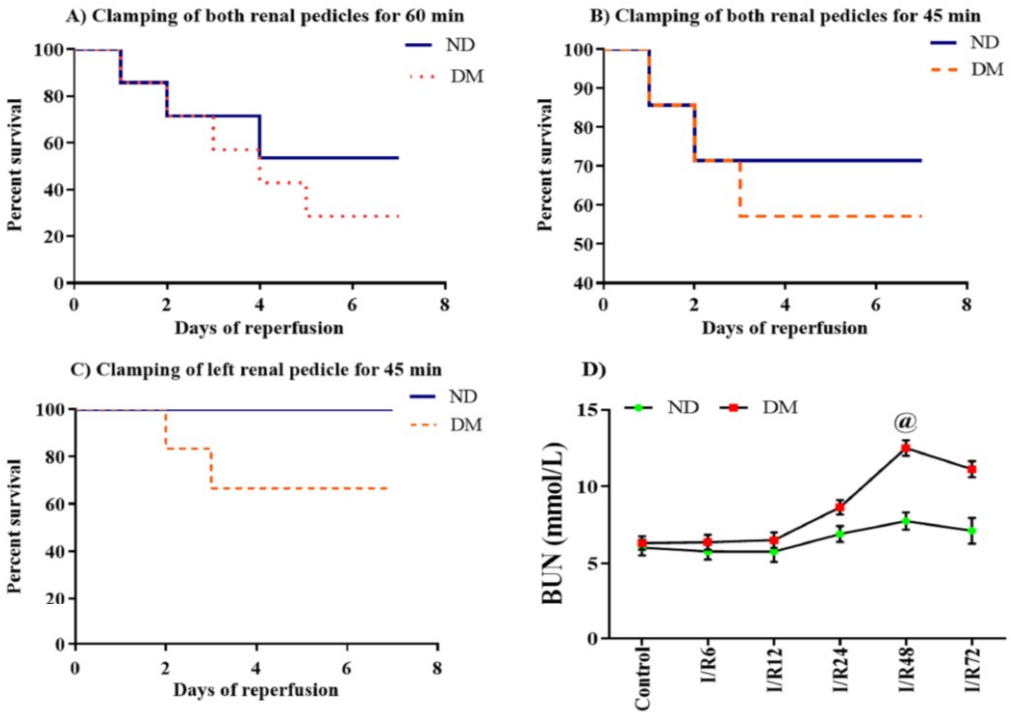

Figure 5.1 Survival of diabetic rats and non-diabetic rats after ischemic-AKI.

Diabetic rats and non-diabetic rats were subjected to 60 or 45 min of bilateral renal ischemia along with 45 min of unilateral renal ischemia followed by reperfusion at different time-points (6, 12, 24, 48, and 72 hours). Animal survival was recorded for 1 week. Note: Each data is represented as mean ± SD (n=8). (@) P < 0.05 vs. ND-I/R; I/R: Ischemia/reperfusion.

After 4 days of the gradual reduction in the percentage survival rate, ND rats have not shown mortality. However, DM rats showed a gradual reduction in the survival rate of up to 5 days ***(Figure 5.1 A)***. Further, we reduced the ischemic time from 60 min to 45 min and we still observed a gradual loss of animals between 1 to 4 days ***(Figure 5.1 B)***. These results confirm that ischemic AKI led to notably higher death in DM rats compared with ND rats.

In the next pilot study, we tried a unilateral model of AKI by clamping the left renal pedicle for 45 min. All ND rats survived during the observation period of 1 week. In STZ diabetic rats, there was a significant reduction in animals' death ***(Figure 5.1 C)***. Here, we checked the levels of BUN at different time-points (6, 12, 24, 48, and 72 hours), and we found a significant elevation in BUN levels at 48 h time-point ***(Figure 5.1 D)***. Therefore, we continued our first and second objectives with a 48 h time-point.

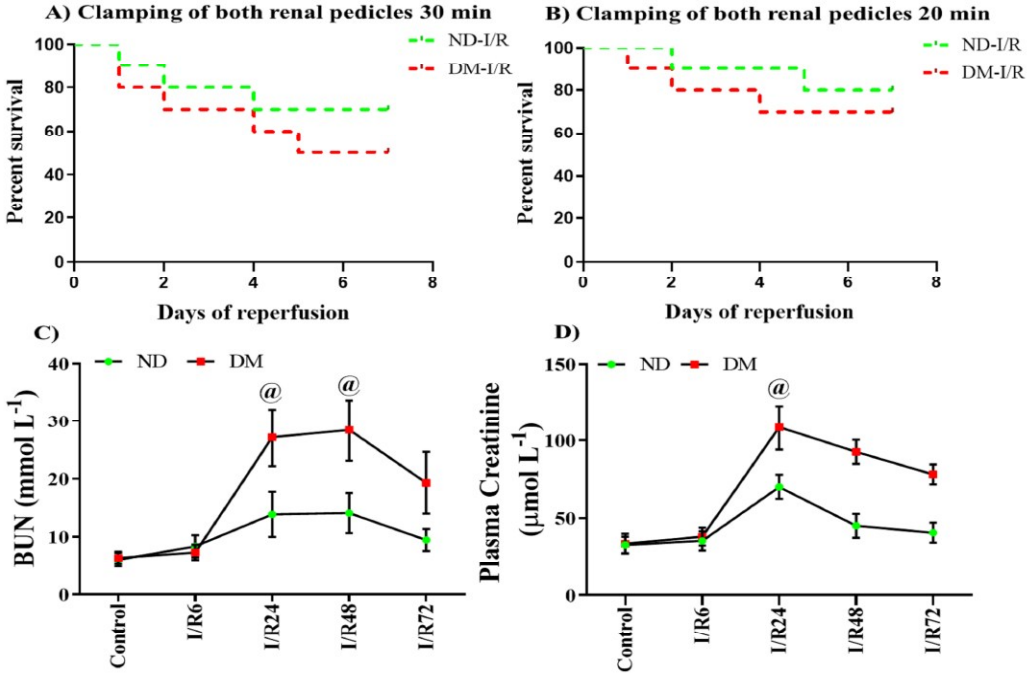

Figure 5.2 Survival of diabetic rats and non-diabetic rats after bilateral ischemia renal injury and estimation of renal functions.

Diabetic rats and non-diabetic rats were subjected to 30 or 20 min of bilateral renal ischemia followed by different time-points of reperfusion (6, 12, 24, 48, and 72 hours). Animal survival was recorded for 1 week. Note: Each data is represented as mean ± SD (n=8). (@) P < 0.05 vs. ND-I/R; I/R: Ischemia/reperfusion.

In the third objective, we utilized the bilateral renal ischemia-reperfusion injury model to study AKI-associated distant organ dysfunction. Here, we carried out 30 or 20 min of ischemia by clamping both renal pedicles. Animals with 30 min of bilateral IRI showed a drastic decline in the survival rate as compared to 20 min of bilateral IRI ***(Figure 5.2 A, B)***. Additionally, the BUN levels were found to reach a peak between 24 and 72 h following reperfusion. While PCr levels remain at peak with 24 h of reperfusion ***(Figure 5.2 D).***

5.2. Epigenetic regulation of inflammatory gene expressions by SET7/9 in IRI under normal and hyperglycemic conditions.

5.2.1. Alteration in the renal functional parameters of diabetic and non-diabetic ischemic rats

STZ administration in rats results in the development of type 1 diabetes. We found that plasma glucose levels of DM and DM-I/R rats remain significantly higher compared to ND and ND-I/R rats ***(Figure 5.3 A)***. BUN levels were found to be elevated in ND-IRI and DM-IRI rats as compared to their respective controls. However, DM-IRI rats showed significant elevation in BUN levels than ND-IRI rats ***(Figure 5.3 B)***. PCr levels were found to be elevated in DM-IRI rats, but not significantly increased compared to ND-IRI rats ***(Figure 5.3 C)***.

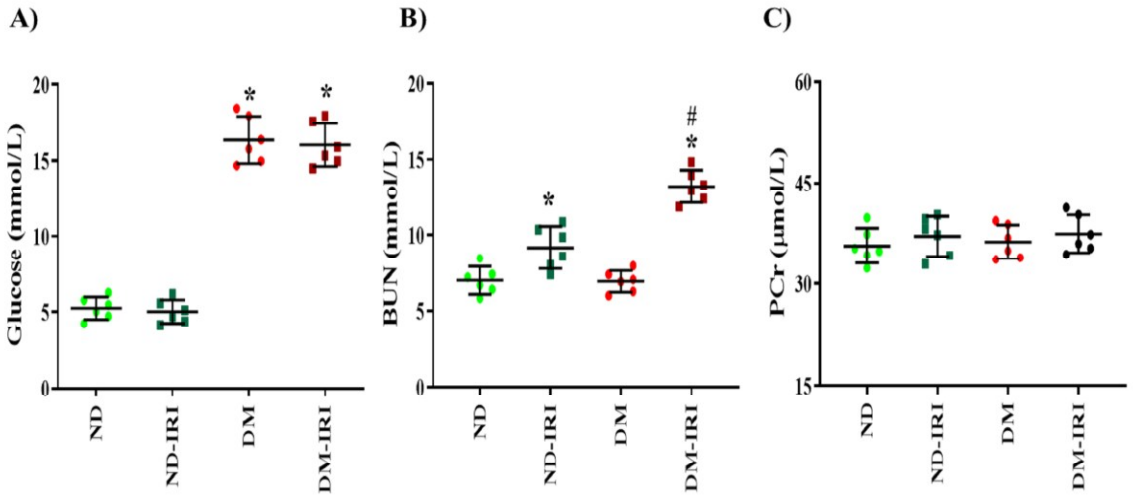

Figure 5.3 Plasma Biochemistry

A-C: Representative scattered plots of plasma glucose (PGL) (A), blood urea nitrogen (BUN) (B), creatinine (PCr) (C). Data are represented as mean ± S.D. (n=6). For statistical comparison, one-way ANOVA with Tukey's multiple comparison test was used where (*) $p < 0.05$ vs ND; (#) $p < 0.05$ vs DM; (@) $p < 0.05$ vs ND-IRI.

5.2.2. Hyperglycemia increases inflammatory cascade following ischemic renal injury

Under the pathogenesis of AKI, the plethora of inflammatory response has been elucidated as the primary mechanism of IRI (Rabb et al., 2016). In the present study, isolated proximal tubules from DM and ND ischemic kidneys showed active NF-κB signaling demonstrated by elevated protein expression of p-NF-κB (S536) and decreased IκBα expression (a

negative regulator of NF-κB), when compared to their respective controls ***(Figure 5.4 A-C)***. In comparison to ND-IRI rats, DM-IRI rats showed significantly higher and diminished expressions of p-NF-κB (S536) and IκBα, respectively. In addition, we also observed markedly increased mRNA levels of *Nfkb p65* in DM-IRI rats in comparison to ND-IRI rats ***(Figure 5.4 E)***. Further, we have checked the protein (MCP-1) expression of down-stream inflammatory signaling molecules in ND and DM groups of rats. We have found a marked elevation in MCP-1 protein expression in DM-IRI and ND-IRI rats as compared to DM and ND rats ***(Figure 5.4 A, D)***.

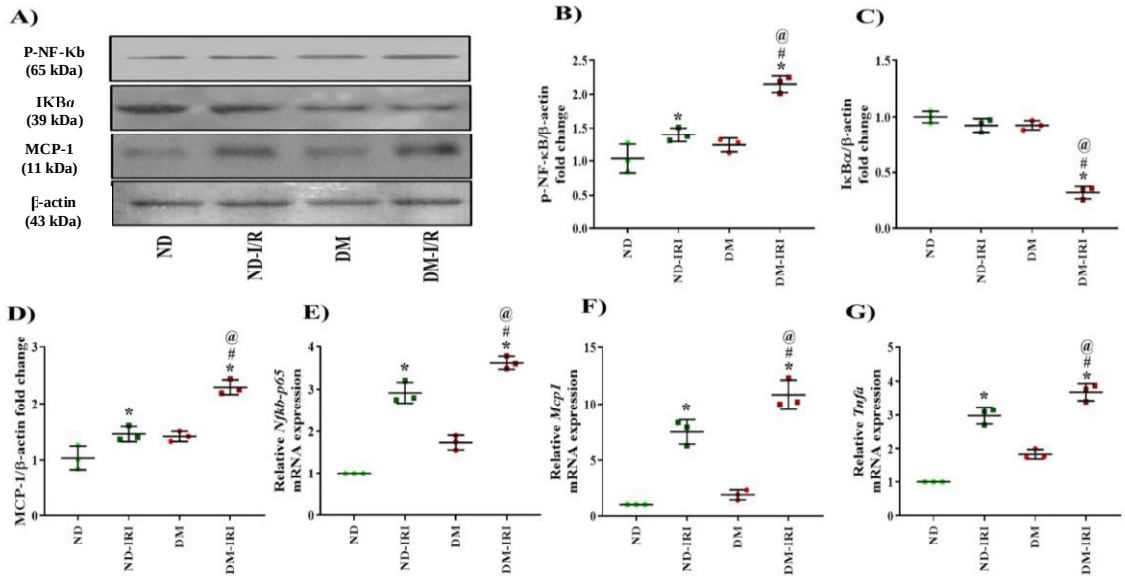

Figure 5.4 Effect of hyperglycemia on protein and mRNA expressions of inflammatory markers following IRI.

A-D: Immunoblots for protein expressions of inflammatory markers in the isolated renal the proximal tubular fraction with β-actin as a loading control (A). Immunoblots were quantified by densitometry analysis e.g. p-NF-κB(S-536) (B), IKBα (C), MCP-1 (D). E-G: mRNA expression of NF-κB, Mcp1, and Tnfa was assessed by qRT-PCR in isolated proximal tubules. 18s rRNA expression was used as an internal control. Data are represented as mean ± S.D. from three independent experiments. For statistical comparison, one-way ANOVA with Tukey's multiple comparison test was used where (*) $p < 0.05$ vs ND; (#) $p < 0.05$ vs DM; (@) $p < 0.05$ vs ND-IRI.

Although, DM-IRI rats showed marked upregulation of MCP-1 protein expression than ND-IRI rats. We checked the mRNA expressions of *Mcp1* and *Tnfa*, we found that DM-IRI and ND-IRI rats showed elevated mRNA expressions of *Mcp1* and *Tnfa* as compared

to DM and ND rats, respectively ***(Figure 5.4 F-G)***. Whereas DM-IRI rats showed significant elevation in *Mcp1* and *Tnfa* mRNA expressions compared to ND-IRI rats. Therefore, in comparison to ND rats, DM rats are more susceptible to inflammatory response under IRI.

5.2.3. Hyperglycemia alters histone ubiquitination in isolated proximal tubules of ischemic kidney

Epigenetic machinery exerts a substantial role in the pathogenesis of AKI (Fontecha-Barriuso et al., 2018). In the present study, we perceived a significant increase in H2AK119Ub and H2BK120Ub expression in diabetic and non-diabetic ischemic rats (***Figure 5.5 A-C***). However, DM-IRI rats showed significant elevation in H2AK119Ub and H2BK120Ub expression than ND-IRI rats. Dysregulation of UPS has been described in diabetic cardiovascular and renal complications (Goru et al., 2016; Kadakol et al., 2015). Thus, the increased expression of H2A and H2B ubiquitination in IRI may relate to the variations in histone specific UPS components, E3 ligases, and DUBs. In this study, we found alterations in the expression of epigenetic enzymes that control some of the IRI-altered histone modifications in ND-IRI and DM-IRI rats. *Rnf2*, E3 ligases specific for H2AK119 and H2BK120 monoubiquitination, are found to be increased in ischemic diabetic and non-diabetic rats compared to their respective controls (***Figure 5.5 D***). Among both groups, ischemic DM rats have shown marked upregulated mRNA levels of *Rnf2* compared to ischemic ND rats (***Figure 5.5 E-G***). In proximal tubules isolated from ischemic kidneys, we found a marked reduction in the mRNA expression of DUBs specific to histone H2A and H2B ubiquitination (*Usp 16*, *21,* and *22*) (***Figure 5.5 E-G***). However, ischemic DM rats had shown a drastic decrease in DUBs mRNA levels compared to ischemic ND rats (***Figure 5.5 E-G***) (Goru et al., 2017a).

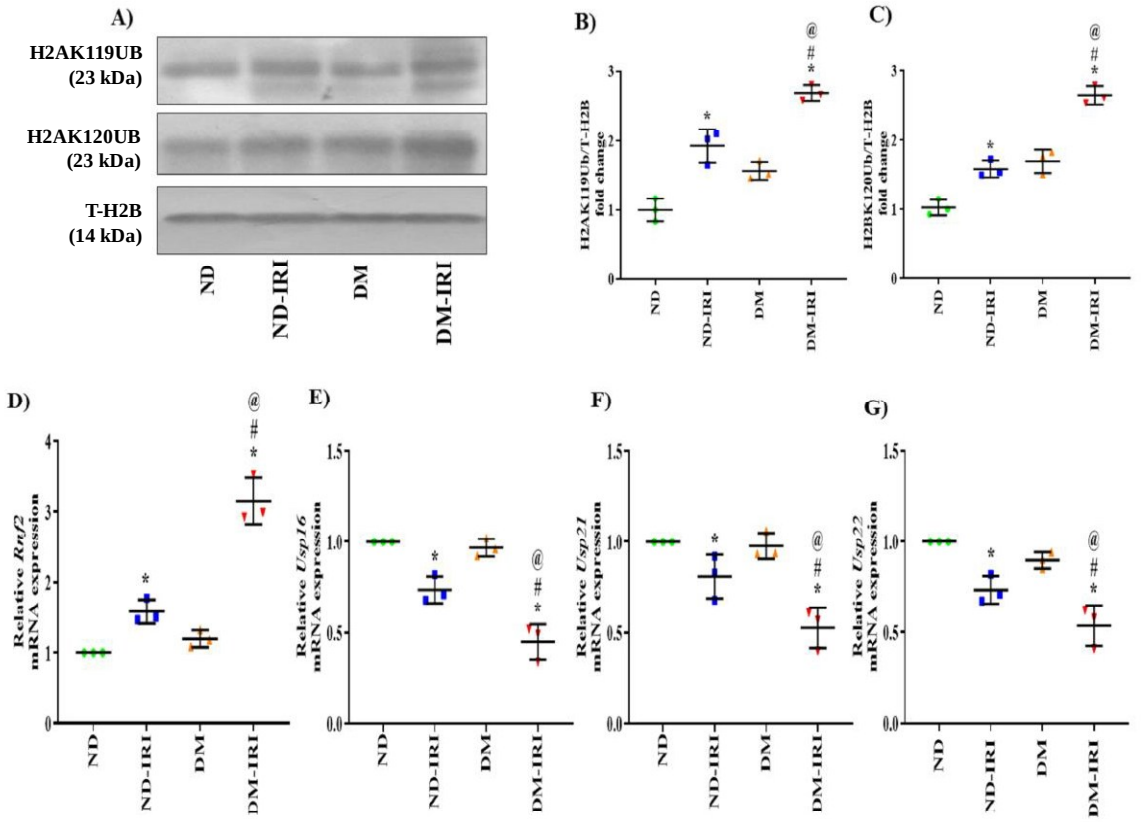

Figure 5.5 Expression of H2AK119Ub, H2BK120Ub, and mRNA expressions of Rnf2, Usp16, Usp21, Usp22 in isolated proximal tubules of ischemic kidney obtained from diabetic and non-diabetic rats.

A-C: (A) Western blot analysis of H2AK119Ub, H2BK120Ub. (B, C) Quantitative analysis of H2AK119Ub, H2BK120Ub. D-G: mRNA expressions of Rnf2, Usp16, Usp21, Usp22 was assessed by qRT-PCR in isolated proximal tubules. 18s rRNA expression was used as an internal control. Data are represented as mean ± S.D. from three independent experiments. For statistical comparison, one-way ANOVA with Tukey's multiple comparison test was used where (*) $p < 0.05$ vs ND; (#) $p < 0.05$ vs DM; (@) $p < 0.05$ vs ND-IRI.

5.2.4. Hyperglycemia alters histone H3 dimethylation in isolated proximal tubules of ischemic kidney

In the present study, we have checked the expression of histone H3K4Me2, H3K9Me2, and H3K36Me2 in the isolated proximal tubules. We found that permissive histone methylation marks i.e. histone H3K4Me2 and H3K36Me2 were significantly elevated in isolated proximal tubules of DM-IRI and ND-IRI rats compared to respective controls ***(Figure 5.6 A, B, D)***. However, diabetic rats underwent IRI showed marked elevation of

histone H3K4Me2 and H3K36Me2 expressions compared to non-diabetic rats who underwent IRI ***(Figure 5.6 A, B, D)***. Further, H3K9Me2 expression (repressive histone methylation mark) was observed to be decreased in ischemic DM and ND rats. Even though, DM-IRI rats showed profound alterations in histone di-methylation at H3K9 as compared to ischemic ND-IRI rats ***(Figure 5.6 A, C)***.

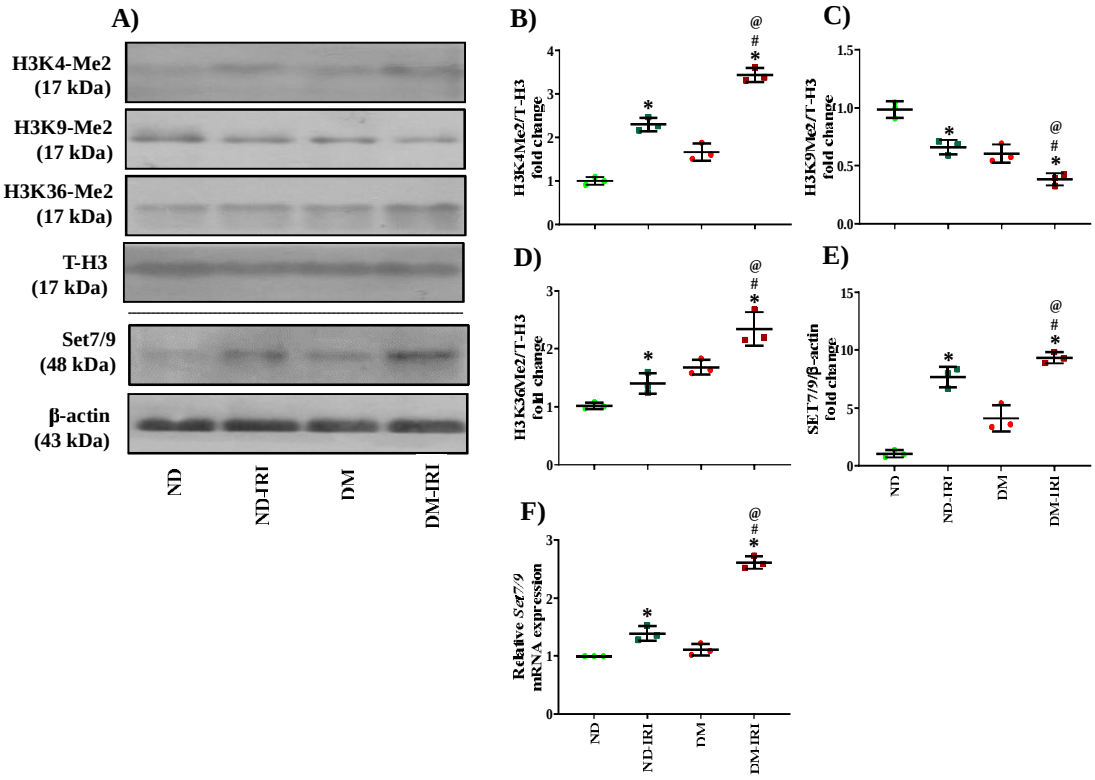

Figure 5.6 Expression of H3K4Me2, H3K36Me2, H3K9Me2, and SET7/9 in isolated proximal tubules of ischemic kidney obtained from diabetic and non-diabetic rats.

A-E: (A) Western blot analysis of H3K4Me2, H3K9Me2, H3K36Me2, and SET7/9. (B, C, D, E) Quantitative analysis of H3K4Me2, H3K9Me2, H3K36Me2, and SET7/9. F: mRNA expression of Set7/9. was assessed by qRT-PCR in isolated proximal tubules. 18s rRNA expression was used as an internal control. Data are represented as mean ± S.D. from three independent experiments. For statistical comparison, one-way ANOVA with Tukey's multiple comparison test was used where (*) $p < 0.05$ vs ND; (#) $p < 0.05$ vs DM; (@) $p < 0.05$ vs ND-IRI.

5.2.5. Hyperglycemia upregulates the protein and mRNA expression of H3K4 specific histone methyltransferase-SET7/9 in ischemic renal injury

Histone methyltransferases (HMTs) play a crucial role in chromatin remodeling and gene expression (Fontecha-Barriuso et al., 2018). In our study, we found that protein and mRNA expression of H3K4Me2-specific methyltransferase, SET7/9 was highly upregulated after ischemic insult in DM and ND rats ***(Figure 5.6 A, E-F***). Interestingly, DM-IRI rats showed significantly elevated protein and mRNA expressions of SET7/9 as compared to ND-IRI rats ***(Figure 5.6 A, E-F).***

5.2.6. Effect of Cyproheptadine on renal biochemistry in diabetic and non-diabetic rats upon ischemic renal injury

In this study, Cyproheptadine treatment was administered using low (10 mg/kg/day, *i.p.*) and high (20 mg/kg/day, *i.p.*) doses in DM-IRI and ND-IRI rats. None of the therapy has any effect on plasma glucose of DM-IRI compared to DM rats ***(Figure 5.7 A)***.

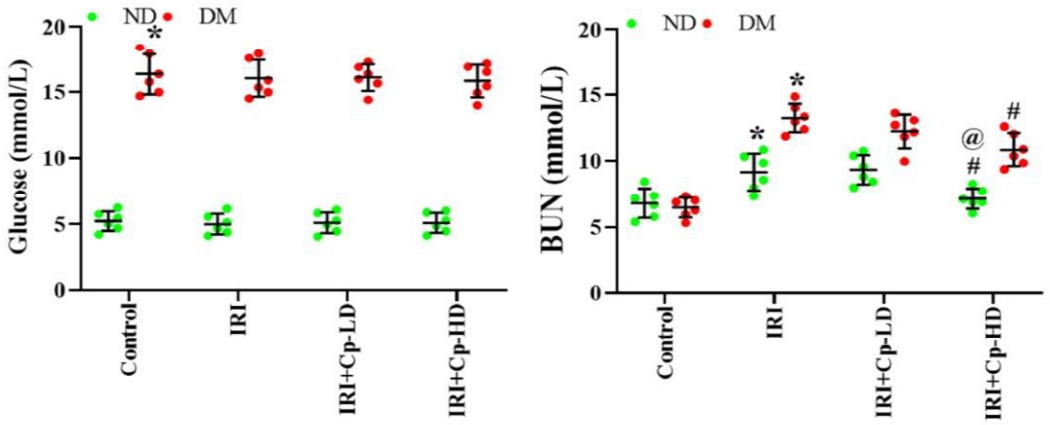

Figure 5.7 Cyproheptadine improves the renal function associated with IRI.

A-B: Representative scattered plots of plasma glucose (PGL) (A), blood urea nitrogen (BUN) (B). Data are represented as mean ± S.D. (n=6). For statistical comparison, two-way ANOVA with Tukey's multiple comparison test was used where (*) $p < 0.05$ vs control; (#) $p < 0.05$ vs IRI; (@) $p < 0.05$ vs IRI-Cp-LD.

Furthermore, in the ND group, we found that elevated BUN levels were significantly attenuated by the high dose of Cyproheptadine (ND-IRI+Cp-HD) compared to a low dose of Cyproheptadine (ND-IRI+Cp-LD) and ND-IRI rats ***(Figure 5.7 B)***. In the DM group, a high dose of Cyproheptadine has markedly reduced the BUN levels compared to DM-IRI

rats ***(Figure 5.7 B)***. Among Cp-HD groups, DM-IRI rats showed lesser recovery as compared to ND rats.

5.2.7. Effect of Cyproheptadine on tubular damage in diabetic and non-diabetic rats upon ischemic renal injury

Next, we performed the histopathological evaluation of the kidney cortex by H and E staining. ND-IRI and DM-IRI rats exhibited significantly increased tubular necrosis ***(Figure 5.8 A, B)***.

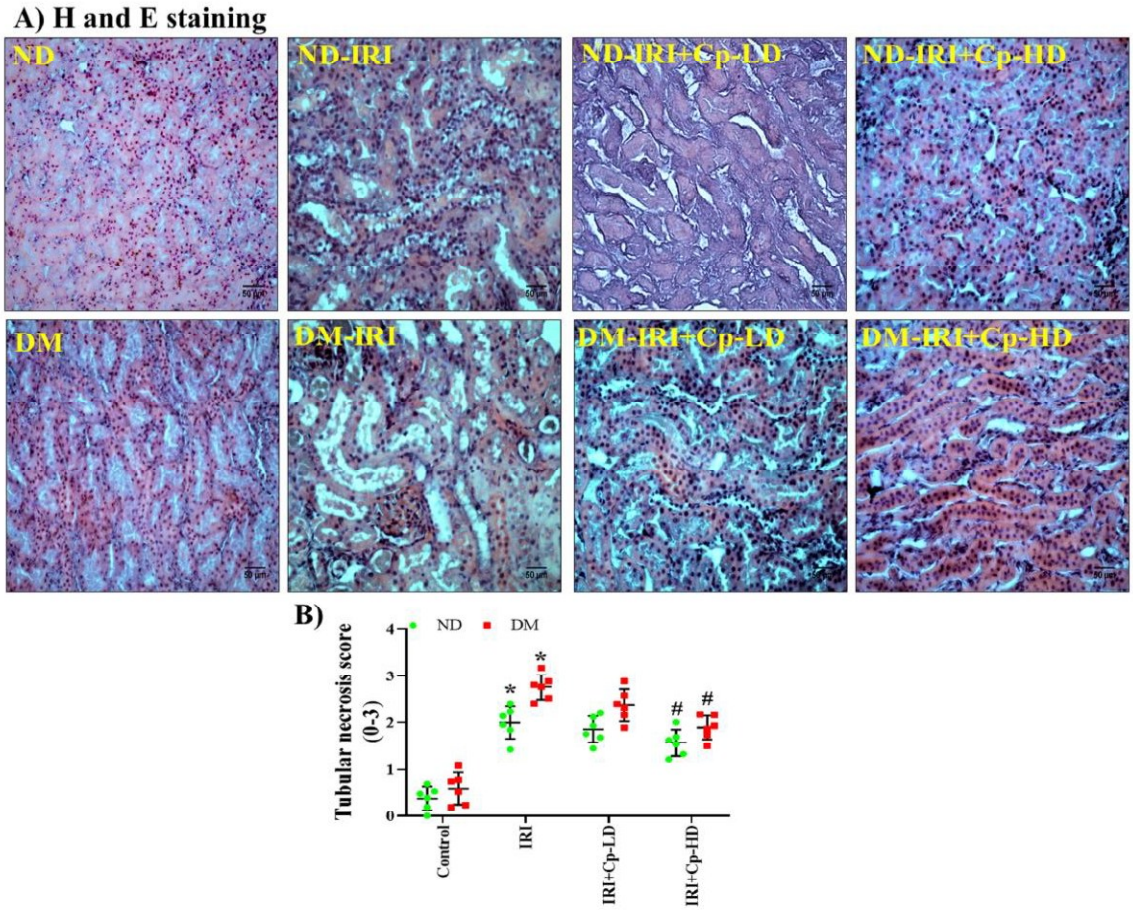

Figure 5.8 Cyproheptadine treatment attenuates tubular necrosis associated with IRI.

Representative images for H and E staining of kidney sections (original magnification 400x and scale bar- 50 µm). At least 4-5 images from each stained kidney section and a total of six different kidneys per group were observed by a blinded observer for tubular necrosis (A). The tubular necrosis was analyzed semi-quantitatively and scored from 0 to 3 (B). Data are represented as mean ± S.D. Two-way ANOVA with Tukey's multiple comparison test was applied for statistical comparison. (*) $p < 0.05$ vs control; (#) $p < 0.05$ vs IRI.

Cyproheptadine in low dose did not exert any significant effect on improving tubular necrosis, however, a high dose of Cyproheptadine produced marked reduction in tubular necrosis in ischemic ND and DM kidneys' ***(Figure 5.8 A, B)***. Therefore, our data suggest that inhibition of SET7/9 prevents tubular damage in ND and DM rats upon IRI.

5.2.8. Effect of Cyproheptadine on renal inflammation and SET7/9 expression in diabetic and non-diabetic rats upon ischemic renal injury

We observed that DM-IRI and ND-IRI rats presented marked elevation of p-NFκB expressions in the renal proximal tubular portion as compared to respective controls ***(Figure 5.9 A, B)***. Here, the DM-IRI group showed higher p-NFκB expressions compared to ND-IRI group (***Figure 5.9 B***). In ND and DM rats, Cyproheptadine high dose (Cp-HD) treatment had significantly reduced the p-NFκB expressions as compared to IRI and low dose group. In the high dose group, ND-IRI rats showed a marked reduction in p-NFκB expressions compared to DM-IRI rats (***Figure 5.9 B***).

Of note, all etiologies share one common feature, where proximal tubular injury accompanied by inflammation and immune activation. MCP-1, a macrophage infiltration marker, impart proximal tubular damage by inducing inflammatory cytokines like IL-1, IL-6, and TNF-α (Kezić et al., 2017). In our study, we observed a significant elevation in MCP-1 protein expression in ischemic kidneys of ND and DM rats (***Figure 5.10 A, B***). treatment with a high dose of Cyproheptadine has significantly attenuated the MCP-1 expression compared to IRI and low dose treated rats (***Figure 5.10 A, B***).

Further, IHC images of kidney tissue revealed the elevated expressions of SET7/9 in ND-IRI and DM-IRI rats. In this, DM-IRI rats showed a significant elevation of SET7/9 expression compared to ND-IRI rats (***Figure 5.11 A, B***). We checked the effect of Cyproheptadine treatment and we found significant amelioration of SET7/9 expression after high dose treatment in ND-IRI and DM-IRI rats. Here, the low-dose of Cyproheptadine also reduced the SET7/9 expression which was not significant (***Figure 5.11 A, B***).

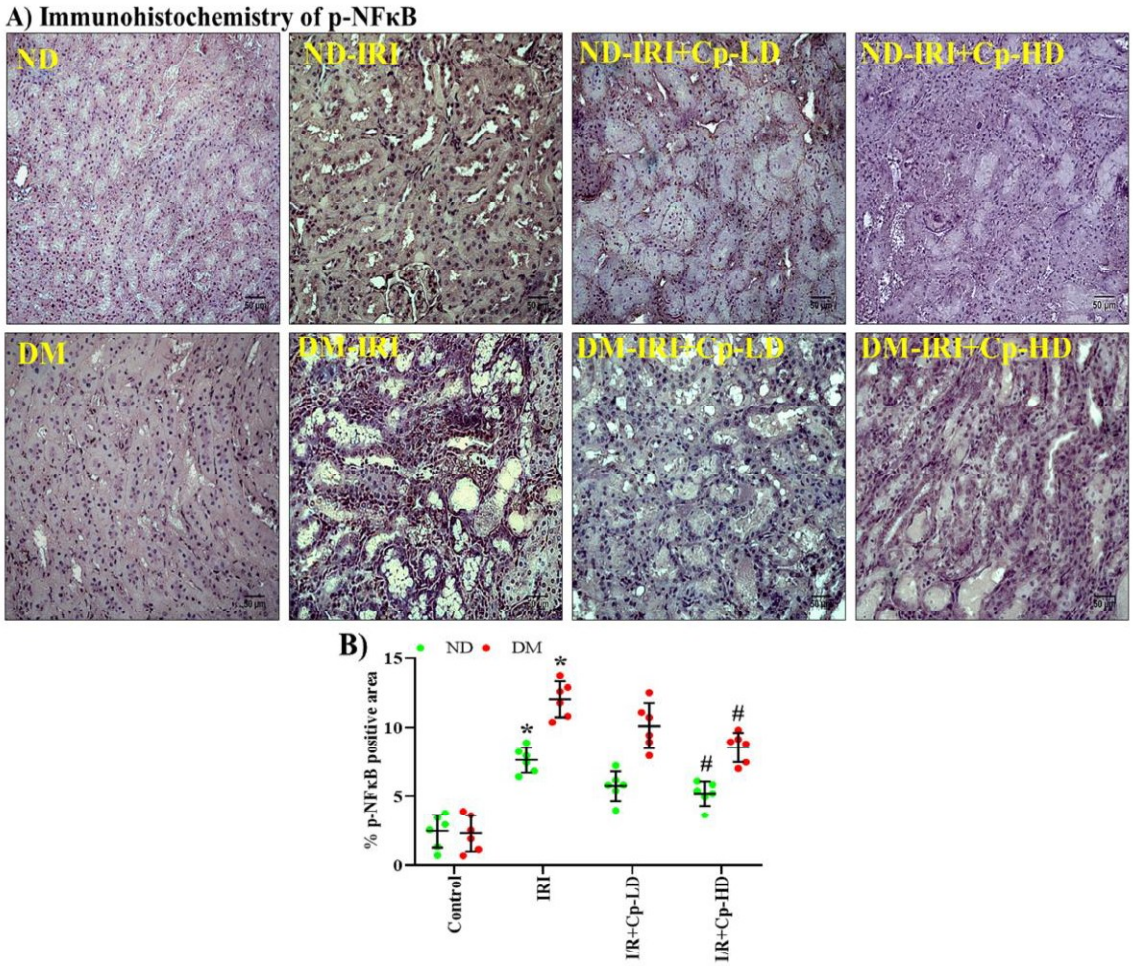

Figure 5.9 Cyproheptadine treatment leads to attenuation of p-NFκB expression in diabetic and non-diabetic rats upon IRI.

A: Representative images of IHC staining for p-NFκB in the kidney tissues (original magnification 400× and scale bar 50µm). Around 4-5 sections from each stained kidney microscopy slide and a total of six different kidney slides per group were seen under a microscope and images were captured. B: Semi-quantitative analysis of all the images via ImageJ (color deconvolution plugin was utilized for analysis) for calculating the DAB-positive area. All Data are represented as mean ± S.D. Two-way ANOVA with Tukey's multiple comparison test was used for statistical comparison. (*) P < 0.05 vs control; (#) P < 0.05 vs IRI.

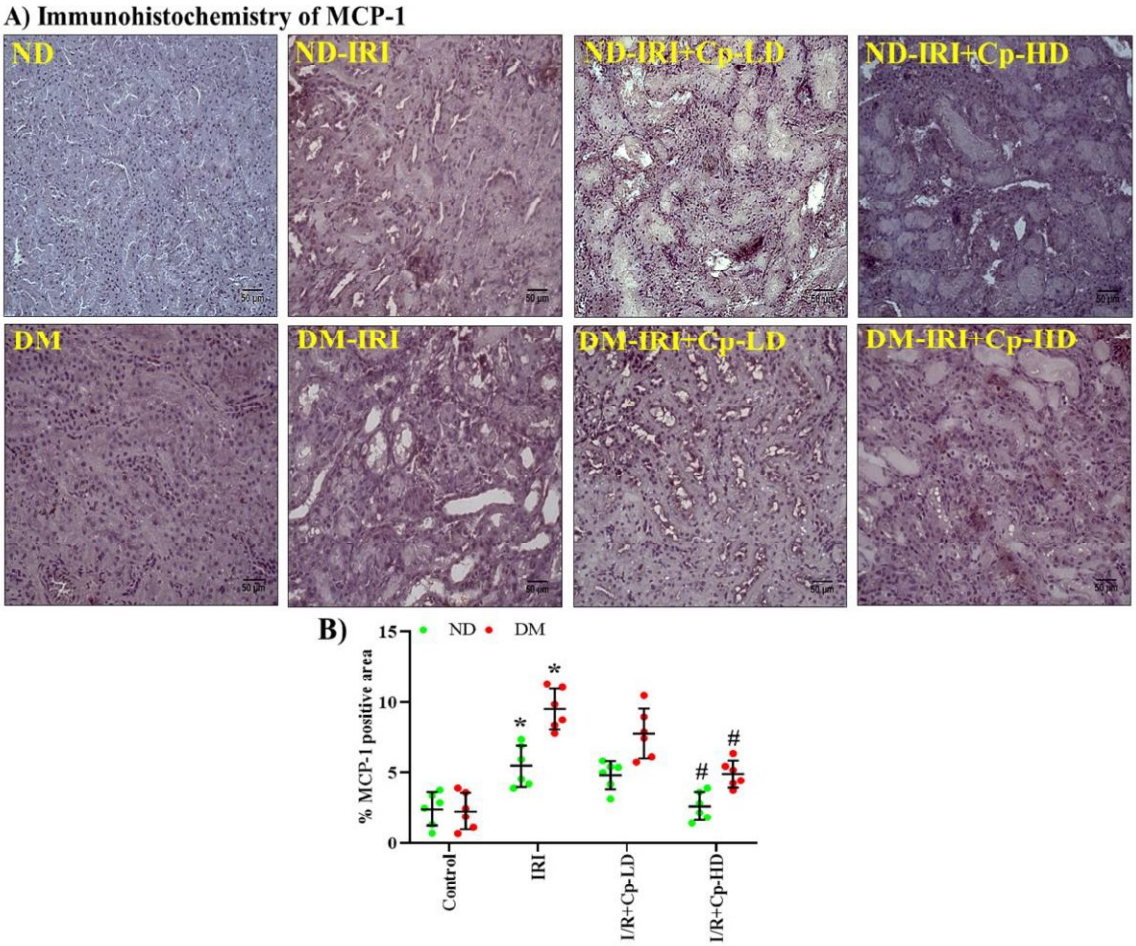

Figure 5.10 Cyproheptadine treatment leads to attenuation of MCP-1 expression in diabetic and non-diabetic rats upon IRI.

A: Representative images of IHC staining for MCP-1 in the kidney tissues (original magnification 400× and scale bar 50µm). Around 4-5 sections from each stained kidney microscopy slide and a total of six different kidney slides per group were seen under a microscope and images were captured. B: Semi-quantitative analysis of all the images via ImageJ (color deconvolution plugin was utilized for analysis) for calculating the DAB-positive area. All Data are represented as mean ± S.D. Two-way ANOVA with Tukey's multiple comparison test was used for statistical comparison. (*) P < 0.05 vs control; (#) P < 0.05 vs IRI.

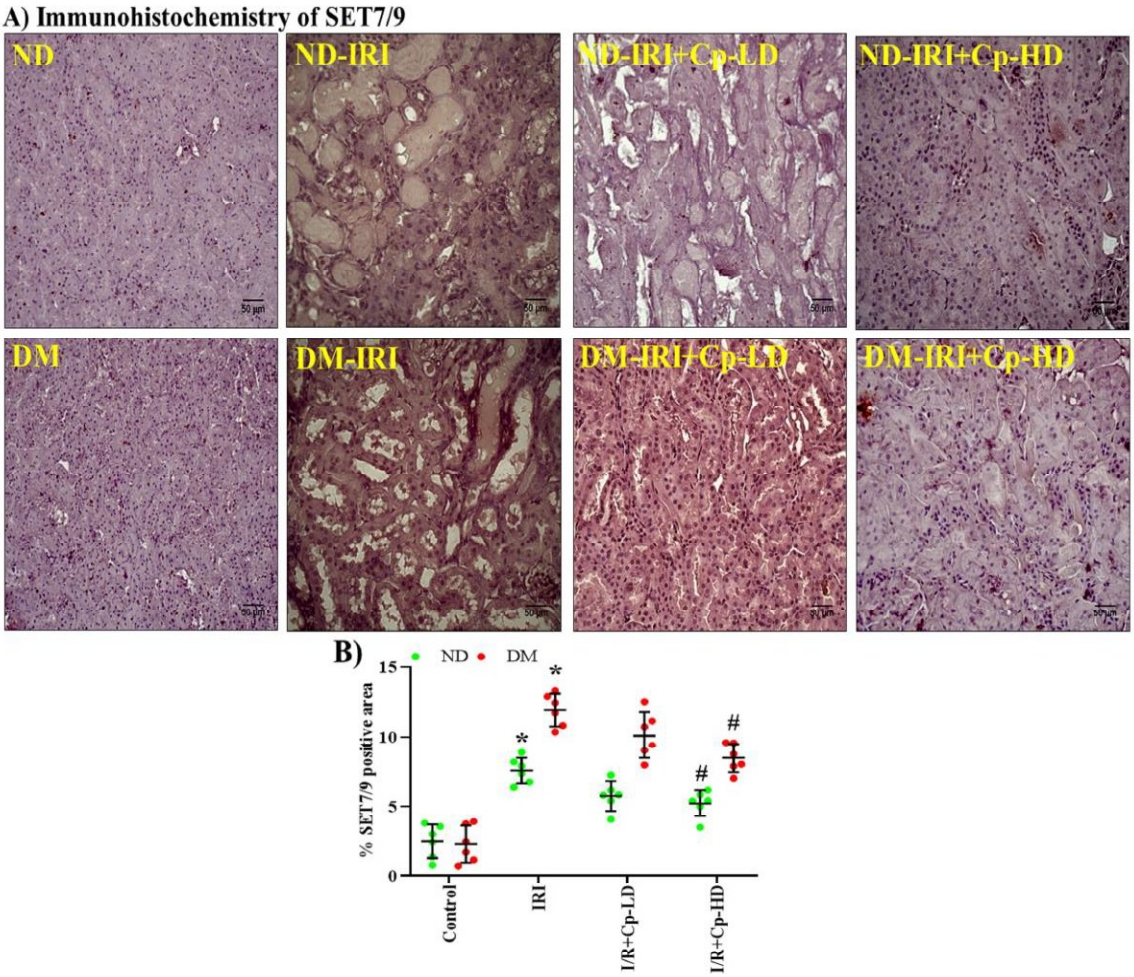

Figure 5.11 Cyproheptadine treatment ameliorated SET7/9 expression in diabetic and non-diabetic rats upon IRI.

A: Representative images of IHC staining for SET7/9 in the kidney tissues (original magnification 400× and scale bar 50µm). Around 4-5 sections from each stained kidney microscopy slide and a total of six different kidney slides per group were seen under a microscope and images were captured. B: Semi-quantitative analysis of all the images via ImageJ (color deconvolution plugin was utilized for analysis) for calculating the DAB-positive area. All Data are represented as mean ± S.D. Two-way ANOVA with Tukey's multiple comparison test was used for statistical comparison. (*) P < 0.05 vs control; (#) P < 0.05 vs IRI.

5.3. Role of AT2R and ACE2 on the progression of IRI under normal and hyperglycemic conditions.

5.3.1. Hyperglycemia increases the severity of the ischemic renal injury

To check the effect of hyperglycemia on IRI, we subjected ND and DM rats to unilateral ischemia followed by reperfusion (I/R) and evaluated the plasma biochemistry and extent of the oxidative stress markers in the isolated proximal tubular fraction. We observed that IRI in ND and DM rats significantly increased BUN levels when compared to respective controls. Interestingly, DM-IRI exhibited augmented BUN levels in comparison to ND-IRI rats. No change was observed in plasma creatinine levels among all the study groups ***(Table 5.1)***. Moreover, IRI in ND and DM rats significantly increased renal tubular oxidative stress, as demonstrated by augmented MDA and GSH levels, nitrate/ nitrite (NO_2/NO_3) ratio, and catalase activity compared to respective controls. Proximal tubules isolated from IR kidneys of DM rats showed significantly higher oxidative stress as compared to ND rats ***(Figure 5.12 A-D)***. Thus, our data indicated IRI hypersensitivity in diabetic rats. Next, we analyzed the expression of proinflammatory cytokines and apoptosis markers by western blot in IRI kidneys from ND and DM rats. IRI augmented tubular inflammation as evinced by increased p-NF-κB and MCP-1 expressions, as well as caused proximal tubular cell apoptosis as demonstrated by increased c-PARP1 and c-Cas-3 expressions when compared to respective controls ***(Figure 5.12 E-I)***. Interestingly, expressions of p-NF-κB, MCP-1, c-PARP1, and c-Cas-3 were significantly higher in IRI kidneys of DM as compared to ND rats ***(Figure 5.12 E-I)***.

Table 5.1 Plasma biochemical parameters

Parameters	**ND**	**ND-IRI**	**DM**	**DM-IRI**
PGl (mmol/L)	4.9 ± 0.18	4.9 ± 0.42	16.9 ± 1.04*	17.3 ± 1.29*
BUN (mmol/L)	7.1 ± 0.71	9.8 ± 0.53*	7.3 ± 0.49	13.8 ± 0.66$^{*, \#}$
PCr (mg/dL)	1.56 ± 0.12	1.59 ± 0.16	1.57 ± 0.19	1.62 ± 0.11

PGL- *plasma glucose,* ***PCr-*** *plasma creatinine,* ***BUN-*** *blood urea nitrogen. Note****:*** *Each data is represented as mean ± S.D. (n=6). (*) P < 0.05 vs. ND; (@) P < 0.05 vs. ND-IRI; (#) P < 0.05 vs. DM; ($) P < 0.05 vs. DM-IRI.*

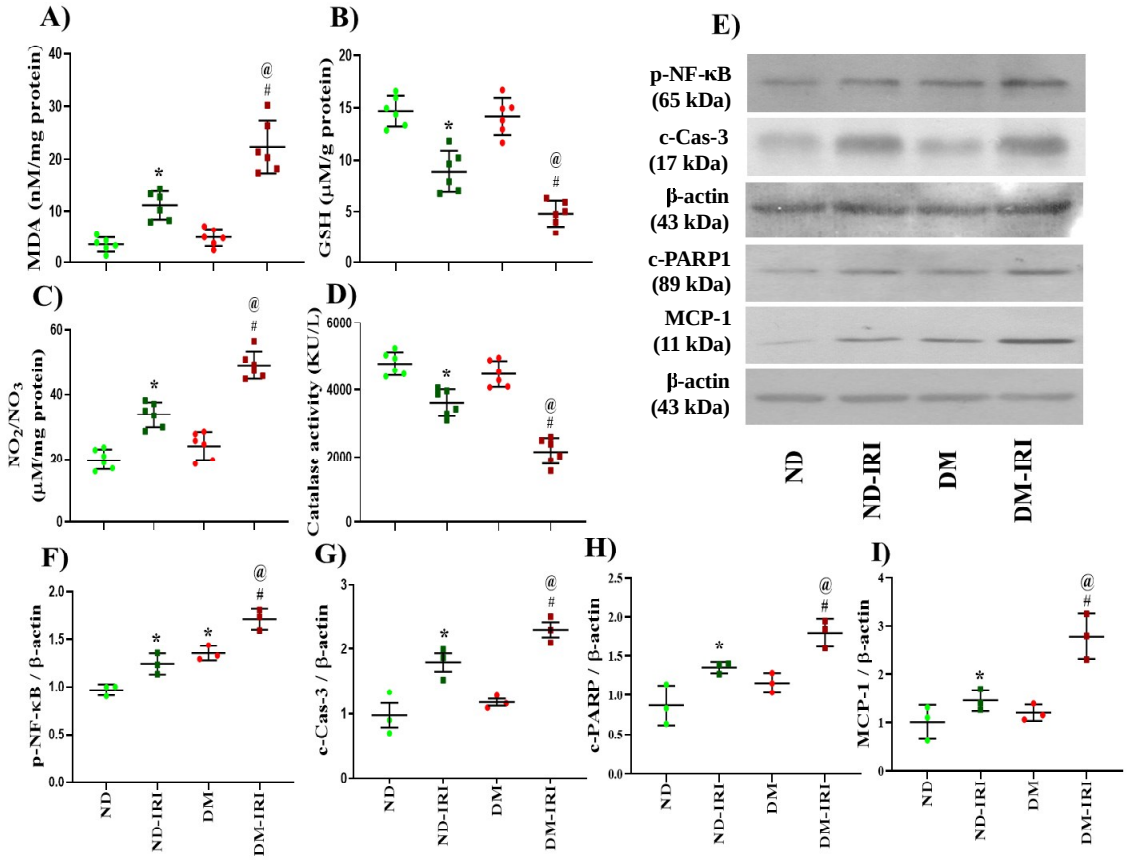

Figure 5.12 Evaluation of oxidative stress, inflammation, and apoptosis in IRI.

A-D: Estimation of oxidative stress markers e.g. malondialdehyde (MDA) (A), GSH (B), NO_2/NO_3 (Griess) (C), catalase activity (D) in kidneys of rats. (n=6). E-I: Immunoblots for protein expressions of inflammatory and apoptotic markers in the isolated renal proximal tubular fraction with β-actin as a loading control (E). Immunoblots were quantified by densitometry analysis e.g. NF-κB(S-536) (F), c-Caspase-3 (G), c-PARP1 (H), and MCP-1 (I). Data are represented as mean ± S.D. from three independent experiments. For statistical comparison, one-way ANOVA with Tukey's multiple comparison test was used where (*) P < 0.05 vs ND; (#) P < 0.05 vs DM; (@) P < 0.05 vs ND-IRI.

Furthermore, we also examined the histopathological alterations persuaded by unilateral renal ischemia in ND and DM rats by H and E staining. Tubular necrosis was observed in the outer cortex of DM-IRI rats and ND-IRI rats; however, DM-IRI rats showed extensive necrosis compared to ND-IRI rats ***(Figure 5.13 A-B)***. These results further confirm the higher susceptibility of the diabetic kidney to IRI-induced AKI.

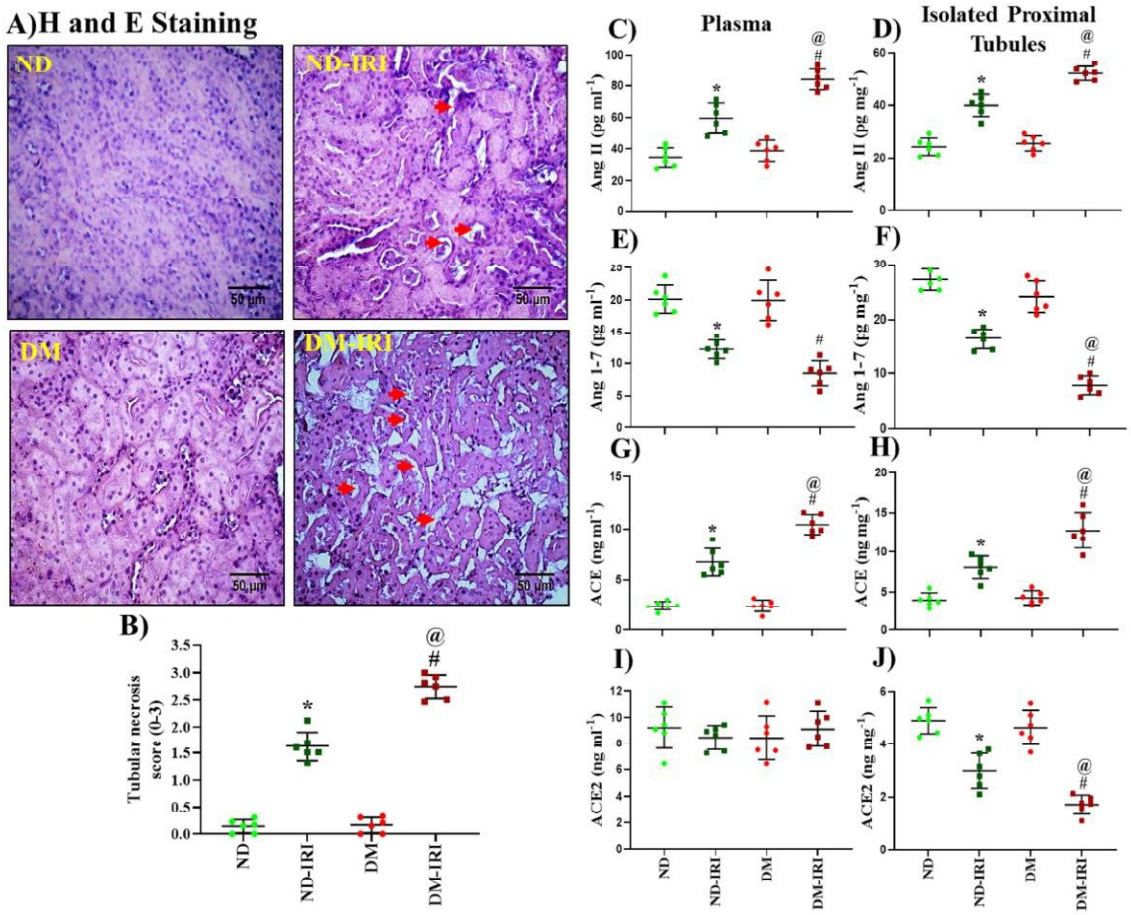

Figure 5.13 IRI modulates tubular necrosis, and systemic and proximal tubular specific ACE, ACE2, Ang II, and Ang (1-7) levels.

A-B: Representative H and E staining images of the cortical region of kidney transverse sections (original magnification 400x and scale bar- 50 µm). At least 4-5 images from each stained kidney section and a total of six different kidneys per group were observed by a blinded observer for tubular necrosis (arrow) (A). The tubular necrosis was analyzed semi-quantitatively and scored from 0 to 3 (B). C-J: Protein expression of ACE, ACE2, Ang II and Ang (1-7) in plasma (C, E, G, I) and isolated proximal tubules (D, F, H, J) was measured by ELISA (n=6). Data are represented as mean ± S.D. For statistical comparison, one-way ANOVA with Tukey's multiple comparison test was used where (*) P < 0.05 vs ND; (#) P < 0.05 vs DM; (@) P < 0.05 vs ND-IRI.

5.3.2. Ischemic renal injury alters systemic and tissue-specific renin-angiotensin system components in non-diabetic and diabetes mellitus rats

We measured the Ang II, Ang (1-7) ACE, and ACE2 levels in plasma and proximal tubular fraction by ELISA kits ***(Figure 5.13 C-J)***. ND-IRI and DM-IRI rats demonstrated increased Ang II and decreased Ang (1-7) levels in plasma and isolated tubules when

compared to ND and DM rats, correspondingly ***(Figure 5.13 C-F)***. Furthermore, IRI to ND and DM rats increased ACE levels in plasma and isolated tubules, whereas decreased ACE2 levels only in isolated tubules with no change in plasma ACE2 levels ***(Figure 5.13 G-J)***. Interestingly, IRI significantly altered the RAS components levels in the DM rats when compared to ND rats.

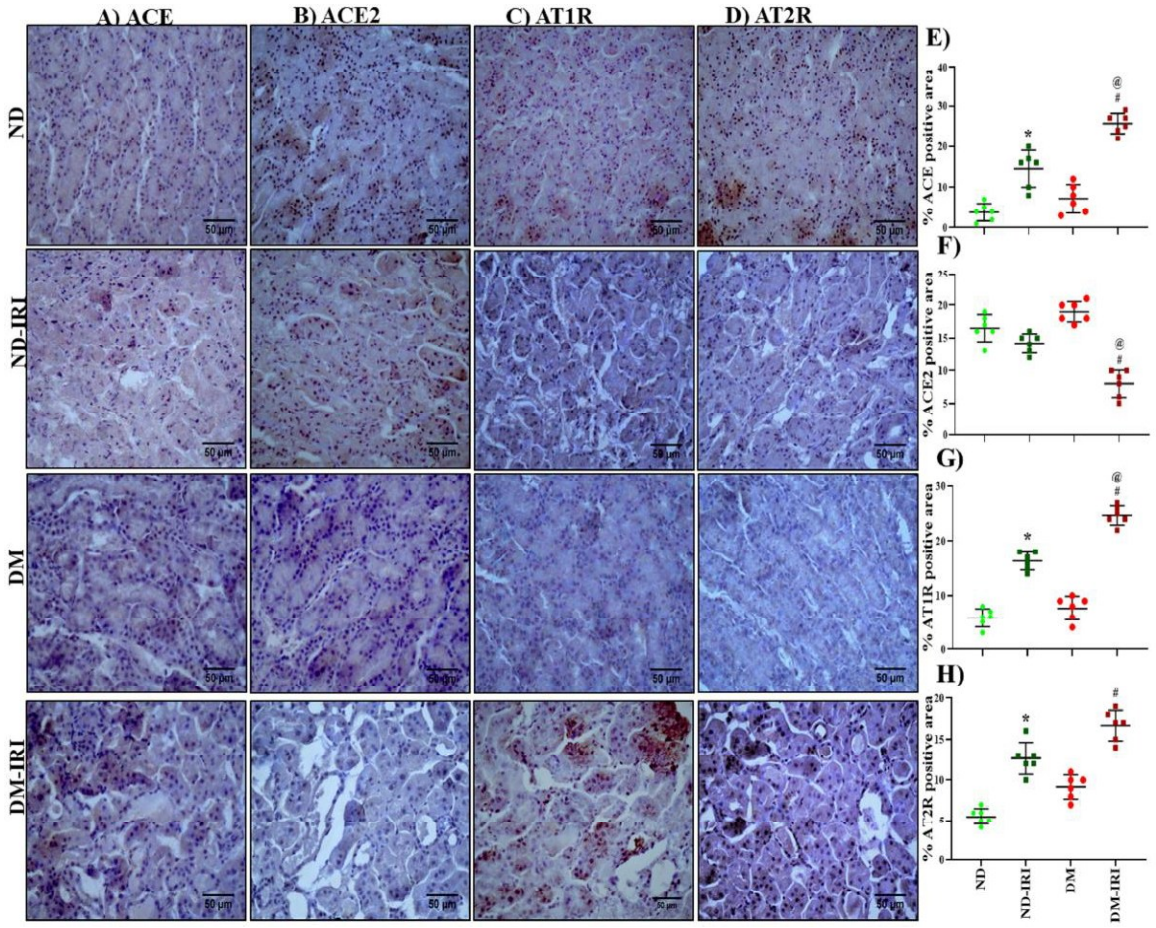

Figure 5.14 Immunohistochemistry for ACE, ACE2, AT1R, and AT2R.

A-D: Representative images of IHC staining for ACE, ACE2, AT1R and AT2R in the cortex of kidney (original magnification 400× and scale bar 50µm). At least 4-5 sections from each stained kidney microscopy slide and a total of six different kidney slides per group were observed under a microscope and images were captured. E-H: Semi-quantitative analysis of all the captured images using ImageJ (color deconvolution plugin was utilized for analysis) for calculating the DAB-positive area (indicates specific protein expressions). All Data are represented as mean ± S.D. One-way ANOVA with Tukey's multiple comparison test, where (*) P < 0.05 vs ND; (#) P < 0.05 vs DM; (@) P < 0.05 vs ND-IRI.

Furthermore, IRI to ND and DM rats increased ACE levels in plasma and isolated tubules, whereas decreased ACE2 levels only in isolated tubules with no change in plasma ACE2

levels ***(Figure 5.13 G-J)***. Interestingly, like our previous observations, IRI significantly altered the RAS components levels in the DM rats when compared to ND rats.

Additionally, IHC revealed increased ACE with no change in ACE2 expressions in IRI kidneys of ND as compared to control rats, whereas IRI kidneys of DM rats demonstrated increased ACE and reduced ACE2 tubular expression in comparison to DM and ND-I/R rats ***(Figure 5.14 A-B, E-F)***. In contrast, renal expression of AT1R and AT2R was significantly augmented in kidneys after IRI as compared to respective controls ***(Figure 5.14 C-D, G-H)***. Moreover, DM-I/R rats' kidneys exhibited increased tubular AT1R expression in comparison to ND-I/R rats' kidneys ***(Figure 5.14 C and G)***. Together our data suggest that the IRI altered the expression of the RAS depressor arm's components in both DM and ND conditions.

5.3.3. AT2R and ACE2 activation improved renal functions, inhibited renal oxidative stress and apoptosis in non-diabetic and diabetes mellitus rats upon ischemic renal injury

Based on our previous results we urged to check the role of RAS depressor arm's modulations on IRI, thus we treated ND-IRI and DM-IRI rats with AT2R agonist (C21, 0.3 mg/kg/day, *i.p.*) and ACE2 activator (Dize, 5 mg/kg/day, *p.o.*), either alone as monotherapy or together as combination therapy.

Table 5.2 Effect of AT2R and ACE2 activation on plasma metabolic parameters.

Parameters	**ND**	**ND-IRI**	**ND-IRI+C21**	**ND-IRI+Dize**	**ND-IRI+CD**	**DM**	**DM-IRI**	**DM-IRI+C21**	**DM-IRI+Dize**	**DM-IRI+CD**
PGL (mmol/L)	6.1 + 0.8	6.3 + 1.0	5.9 ± 0.7	6.9 ± 0.9	6.6 ± 0.6	20.1 + 1.7	19.3 + 1.2	19.8 ± 2.0	18.5 ± 2.4	19.9 ± 0.9
BUN (mmol/L)	6.8 ± 0.3	9.2 ± 0.5*	9.8 ± 0.6	9.5 ± 0.5	7.6 ± 0.4$^{@}$	7.5 ± 0.8	13.3 ± 0.4$^{*,\#}$	12.1 ± 0.5	11.8 ± 0.6	8.7 ± 0.4$^{\$}$

PGL- *Plasma glucose,* ***BUN-*** *Blood urea nitrogen.* ***Note****: Each data is represented as mean ± S.D. (n=6). (*) P < 0.05 vs ND; (#) P < 0.05 vs DM; (@) P < 0.05 vs ND-IRI.*

Plasma biochemistry revealed that AT2R agonist and ACE2 activator combination therapy scientifically lower the BUN levels, whereas monotherapies had no effect on BUN levels in ND-IRI and DM-IRI rats ***(Table 5.2)***.

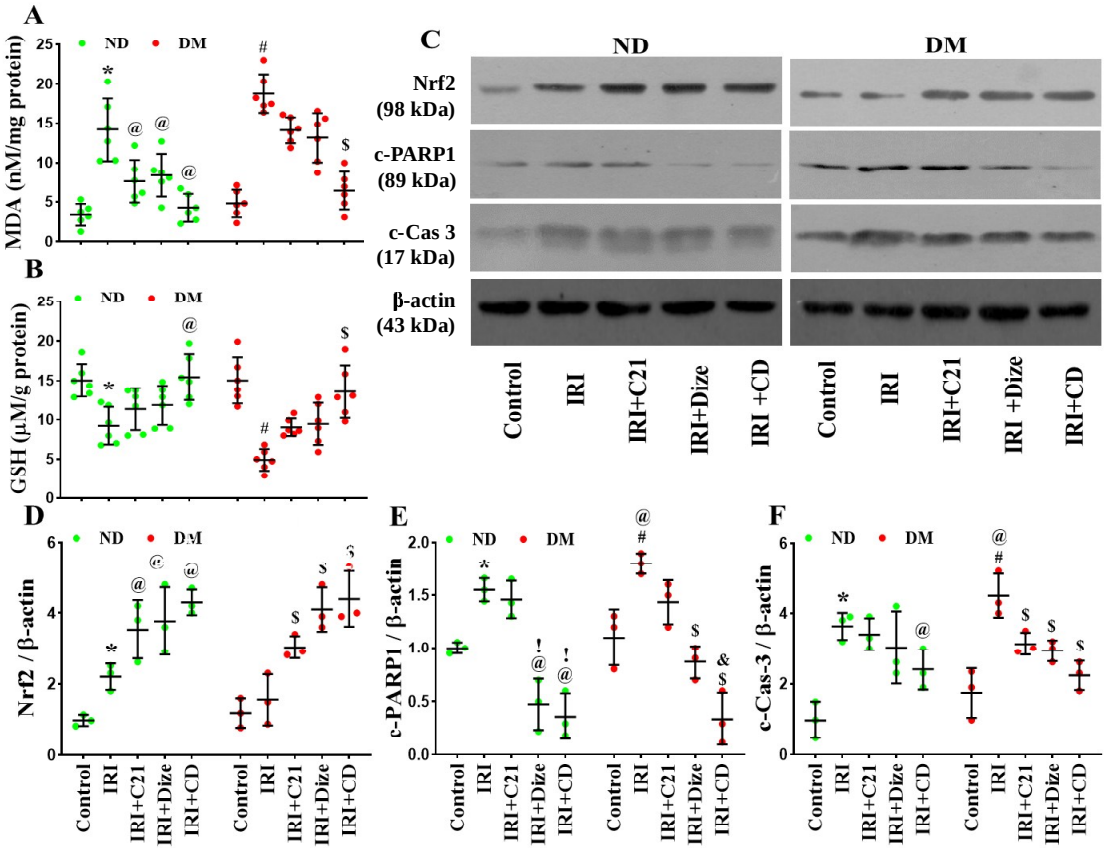

Figure 5.15 AT2R agonist and ACE2 activator protect ND and DM rats against oxidative stress and apoptosis.

A-B: Estimation of oxidative stress markers e.g. malondialdehyde (MDA) (A), GSH (B) in a proximal tubular fraction of rat kidneys (n=6). C-F: Representative western blot images for Nrf2, c-PARP1, c-Cas-3, and β-actin (loading control) protein expressions in isolated proximal tubular fraction (C). Immunoblots were quantified by densitometry analysis e.g. Nrf2 (D), c-PARP1 (E), and c-Cas-3 (F). Data are represented as mean ± S.D. from three independent experiments. One-way ANOVA with Tukey's multiple comparison test for statistical comparison. (*) P < 0.05 vs ND; (@) P < 0.05 vs ND-IRI; (#) P < 0.05 vs DM; ($) P < 0.05 vs DM-IRI; (&) P < 0.05 vs DM-IRI+C21.

C21 and Dize monotherapies to ND-I/R rats reduced MDA and increased Nrf2 expression, with no change in GSH levels. In contrast, both monotherapies could only increase Nrf2 expression in DM-IRI rats and had no effect on MDA and GSH levels. Interestingly,

combination therapy significantly reduced MDA and increased GSH and Nrf2 levels in both ND-IRI and DM-IRI rats ***(Figure 5.15 A-D).*** Next, we checked the expression of apoptosis markers, c-Cas-3, and c-PARP1 by western blot. We found that combination therapy significantly reduced c-Cas-3 and c-PARP1 levels in IRI kidneys of both ND and DM rats ***(Figure 5.15 C, E-F)***.

5.3.4. AT2R and ACE2 activation inhibits renal inflammation and prevented tubular damage in non-diabetic and diabetes mellitus rats upon ischemic renal injury

Inflammation is a hallmark for the IRI (Rabb et al., 2016), thus we analyzed the alteration in the expressions of inflammatory molecules in the tubular fraction of IRI kidneys after AT2R and ACE2 activation.

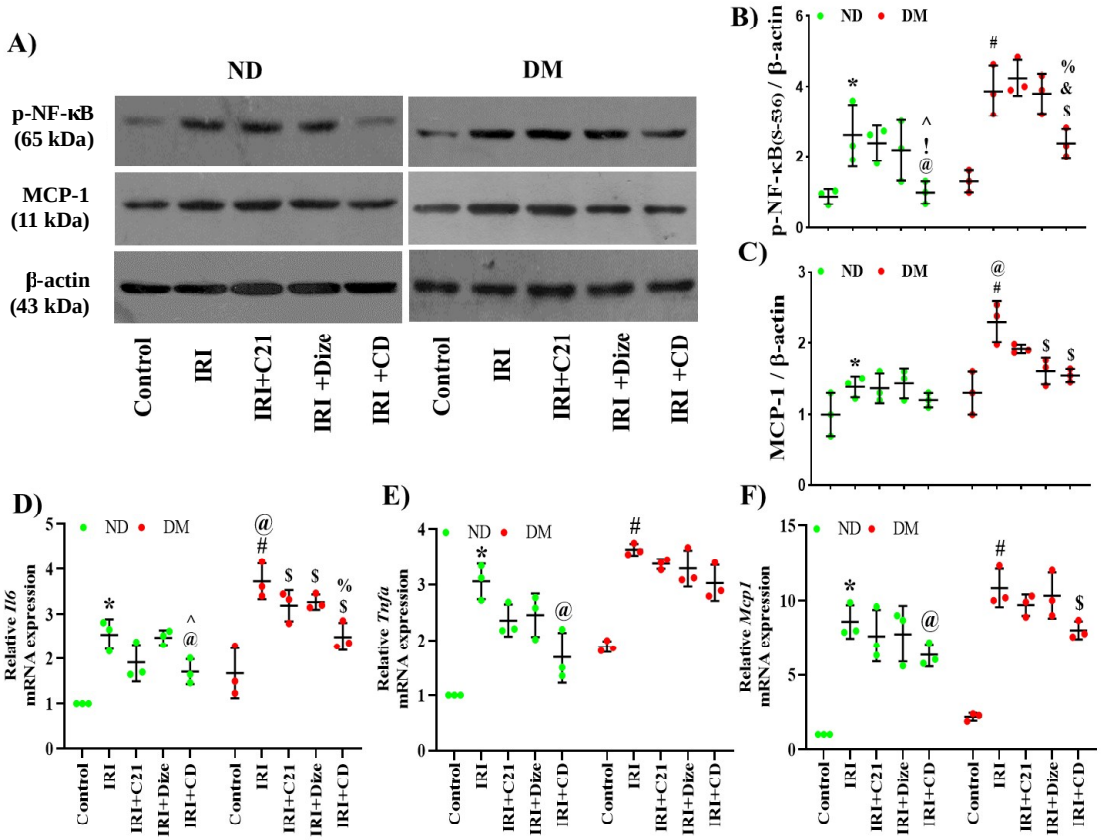

Figure 5.16 Effect of C21, Dize, and their combination therapy on protein and mRNA expressions of inflammatory markers.

A-C: Representative western blot images for protein expressions of p-NF-κB, MCP-1, and β-actin (loading control in isolated proximal tubular fraction (A). Immunoblots were quantified by densitometry analysis e.g. p-NF-κB (B), and MCP-1 (C). D-F: mRNA expression of Il6, Tnfa, and

Mcp1 were assessed by qRT-PCR in isolated proximal tubules. 18s rRNA expression was used as the internal control. Data are represented as mean ± S.D. from three independent experiments. One-way ANOVA with Tukey's multiple comparison test was used for statistical comparison. (*) P < 0.05 vs ND; (@) P < 0.05 vs ND-IRI; (!) P < 0.05 vs ND-IRI+C21; (^) P < 0.05 vs ND-IRI+Dize; (#) P < 0.05 vs DM; ($) P < 0.05 vs DM-IRI; (&) P < 0.05 vs DM-IRI+C21; (%) P < 0.05 vs DM-IRI+Dize.

We observed that IRI increased protein expressions of p-NF-κB and MCP-1 in proximal tubules of ND and DM rats signifying renal inflammation ***(Figure 5.16)***. C21 and Dize monotherapies did not change the expression of p-NF-κB and MCP-1; except Dize monotherapy reduced MCP-1 expression in DM-IRI rats. In contrast, the combination therapy significantly inhibited p-NF-κB and MCP-1 expressions in the tubular fractions of both ND-IRI and DM-IRI rats ***(Figure 5.16 A-C)***.

Furthermore, we found a significant increase in mRNA expressions of *Il6*, *Tnfa,* and *Mcp1* in the tubular fraction of ND and DM rats subjected to IRI ***(Figure 5.16 D-F)***. C21 or Dize monotherapy did not change mRNA expressions of *Tnfa* and *Mcp1* in ND-IRI and DM-IRI rats, whereas reduced *Il6* mRNA expression only in DM-IRI rats. In contrast, combination therapy significantly reduced *Il6* and *Mcp1* mRNA expressions in ND-IRI and DM-IRI rats, while decreased *Tnfa* mRNA expression in ND-IRI with no change in *Tnfa* mRNA expression in DM-IRI rats ***(Figure 5.16 D-F).***

Next, we performed the histopathological evaluation of the kidney cortex by H and E staining. ND-IRI and DM-IRI rats exhibited significantly increased tubular necrosis, which was not prevented by C21 and Dize monotherapies. However, the combination therapy produced marked reduction in tubular necrosis in ischemic ND and DM kidneys' ***(Figure 5.17 A, B)***. Therefore, our data suggest that simultaneous activation of AT2R and ACE2 inhibits renal inflammation and tubular damage in ND and DM rats upon IRI.

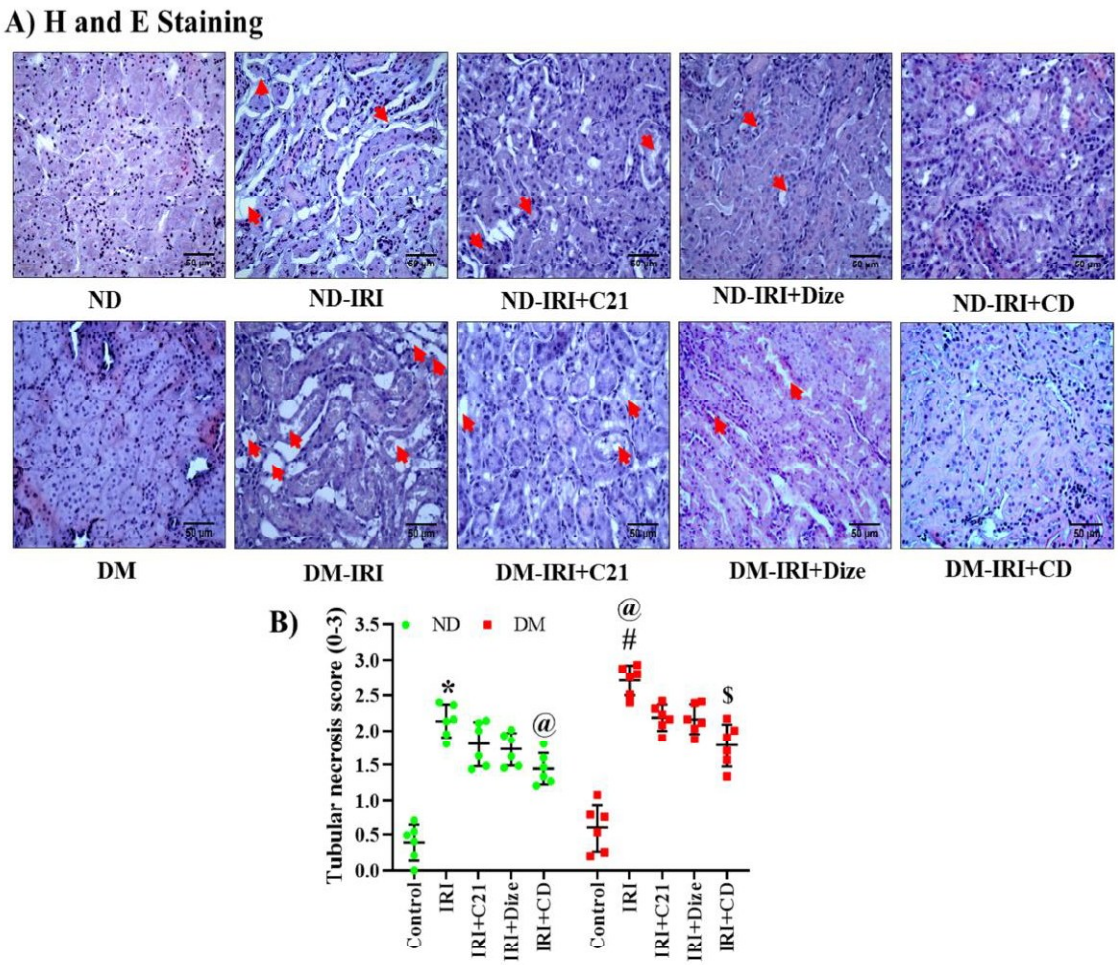

Figure 5.17 AT2R agonist and ACE2 activator prevented tubular necrosis associated with IRI.

Representative images for H and E staining of kidney sections (original magnification 400x and scale bar- 50 µm). At least 4-5 images from each stained kidney section and a total of six different kidneys per group were observed by a blinded observer for tubular necrosis (Red arrow) (A). The tubular necrosis was analyzed semi-quantitatively and scored from 0 to 3 (B). Data are represented as mean ± S.D. One-way ANOVA with Tukey's multiple comparison test was applied for statistical comparison. (*) $p < 0.05$ vs ND; (@) $p < 0.05$ vs ND-IRI; (#) $p < 0.05$ vs DM; ($) $p < 0.05$ vs DM-IRI; (&) $p < 0.05$ vs DM-IRI+C21.

5.3.5. AT2R and ACE2 activation restores the altered systemic and tissue-specific RAS components in non-diabetic and diabetes mellitus rats upon ischemic renal injury

According to our previous results, IRI altered the systemic and tissue-specific RAS components in ND and DM rats. Therefore, next, we checked the effect of AT2R and ACE2

activator treatments on the same. All three-treatment regimen increased tubular ACE2 levels in ND-IRI and DM-IRI rats and reduced plasma ACE levels in DM-IRI rats, while only combination therapy reduced plasma ACE level in ND-IRI rats ***(Figure 5.18 A and F)***. None of the treatment regimens could alter the plasma ACE2 and tubular ACE levels in ND-I/R and DM-I/R rats ***(Figure 5.18 B and E)***. In plasma, Ang II and Ang (1-7) levels remain unchanged after C21 monotherapy, while Ang (1-7) levels significantly increased after Dize monotherapy in ND-IRI and DM-IRI rats. Interestingly, combination therapy significantly reduced Ang II levels and increased Ang (1-7) levels in the plasma of ND-IRI and DM-IRI rats ***(Figure 5.18 C-D)***. In an isolated tubular fraction, all three-treatment regimens significantly reduced Ang II and augmented Ang (1-7) levels in ND-IRI and DM-IRI rats; except C21 monotherapy did not change tubular Ang II and Ang (1-7) levels in ND-IRI rats ***(Figure 5.18 G-H)***. One of the consistent features is that combination therapy was better in normalizing the RAS components levels when compared to respective monotherapies.

Next, we checked mRNA expressions of *At1r, At2r,* and *Masr* in a tubular fraction using qRT-PCR. ND-IRI and DM-IRI rats exhibited increased mRNA expressions of *At1r, At2r,* and *Masr* in a tubular fraction when compared to respective controls. C21 or Dize monotherapy did not change mRNA expressions of *At1r, At2r* and *Masr* in ND-IRI and DM-IRI rats. Interestingly, the combination therapy resulted in a further increase in *At2r* and *Masr* mRNA expressions, with no change in *At1r* mRNA expressions in ND-IRI and DM-IRI rats ***(Figure 5.18 I-K)***. Therefore, our data suggest that the protective effects seen after the combination therapy might relate to the restoration of systemic and tissue-specific RAS components in ND and DM rats upon IRI.

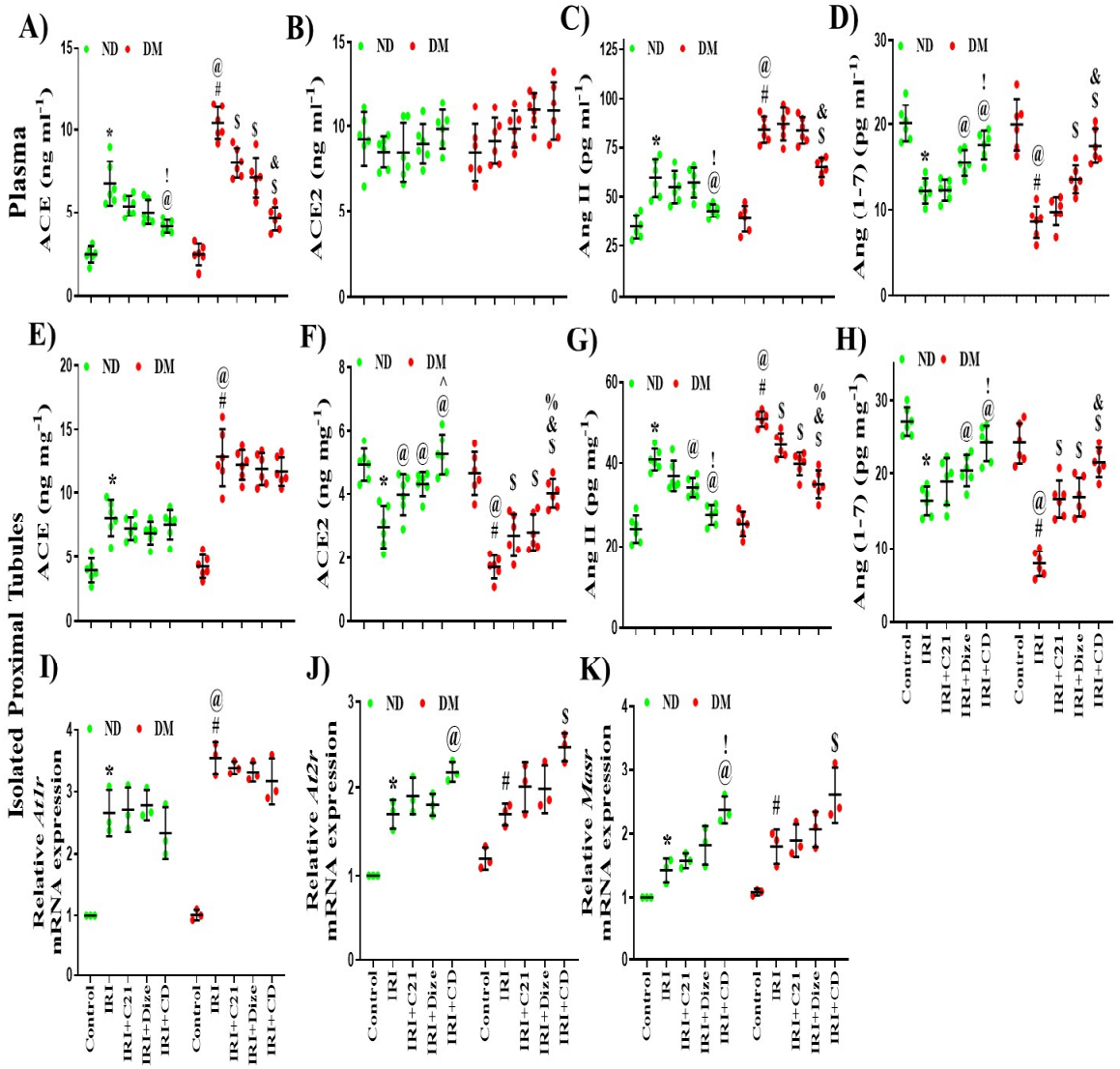

Figure 5.18 Effect of C21, Dize, and their combination therapy on protein and mRNA expressions of RAS components.

A-H: Protein expression of ACE, ACE2, Ang II, and Ang (1-7) in plasma (A-D) and isolated proximal tubules (D-J) was measured by ELISA (n=6). I-K: mRNA expressions of At1r, At2r, and Masr was assessed by qRT-PCR in isolated proximal tubules. 18s rRNA expression was used as the internal control. Data are represented as mean ± S.D. from three independent experiments. One-way ANOVA with Tukey's multiple comparison test was applied for statistical comparison. (*) P < 0.05 vs ND; (@) P < 0.05 vs ND-IRI; (!) P < 0.05 vs ND-IRI+C21; (#) P < 0.05 vs DM; ($) P < 0.05 vs DM-IRI; (&) P < 0.05 vs DM-IRI+C21; (%) P < 0.05 vs DM-IRI+Dize.

5.4. Role of AT2R and ACE2 on the progression of IRI-associated distant organ dysfunction under normal and hyperglycemic conditions.

5.4.1. Hyperglycemia worsens renal functions under ischemic renal injury

In this objective, IRI was induced by bilateral clamping of both renal pedicles for 20 min followed by 24 h of reperfusion. In results, DM rats had increased plasma glucose ***(Figure 5.19 A)*** levels compared to ND rats. Further, we found that IRI in ND and DM rats significantly increased PCr ***(Figure 5.19 B)*** and BUN ***(Figure 5.19 C)*** levels compared to respective controls. DM-IRI rats showed significantly higher BUN and PCr levels compared to ND-IRI rats. Kim-1, a type 1 transmembrane protein, having an immunoglobulin and mucin domain, whose levels are said to be elevated under proximal tubular damage upon ischemic renal injury (Han et al., 2008). In our study, DM-IRI rats showed significantly increased urinary Kim-1 protein levels as compared to ND-IRI rats (***Figure 5.19 D***).

5.4.2. Hyperglycemia impairs locomotor activity and aggravates brain inflammatory mediators after ischemic renal injury

To determine whether the findings of abrupt alterations in kidney functional parameters was accompanied by impaired behavioral parameter and distant organ (brain) cellular inflammation, we checked locomotor activity using actophotometer and performed ELISA for inflammatory molecules like Granulocyte-colony stimulating factor (GCSF) and Glial fibrillary acidic protein (GFAP) in plasma, hippocampus, and cerebral cortex tissue. IRI has a severe effect on the locomotor activity response in DM rats compared to ND rats ***(Figure 5.19 E)***. Further, after IRI, both DM-IRI and ND-IRI had shown an increase in plasma ***(Figure 5.19 F)*** and hippocampal ***(Figure 5.19 G)*** (GCSF levels, compared to their respective controls. However, in comparison to ND-IRI group, DM-IRI group showed a significant increase in GCSF levels in plasma and hippocampus (***Figure 5.19 F, G***). GFAP, an indicator for activated glial cells during brain inflammation, found to get elevated in plasma as well as in the cerebral cortex ***(Figure 5.19 I)*** of DM-IRI and ND-IRI rats. However, DM-IRI rats have shown marked elevation in plasma and cerebral cortex GFAP levels, as compared to ND-IRI rats (***Figure 5.19 H, I***).

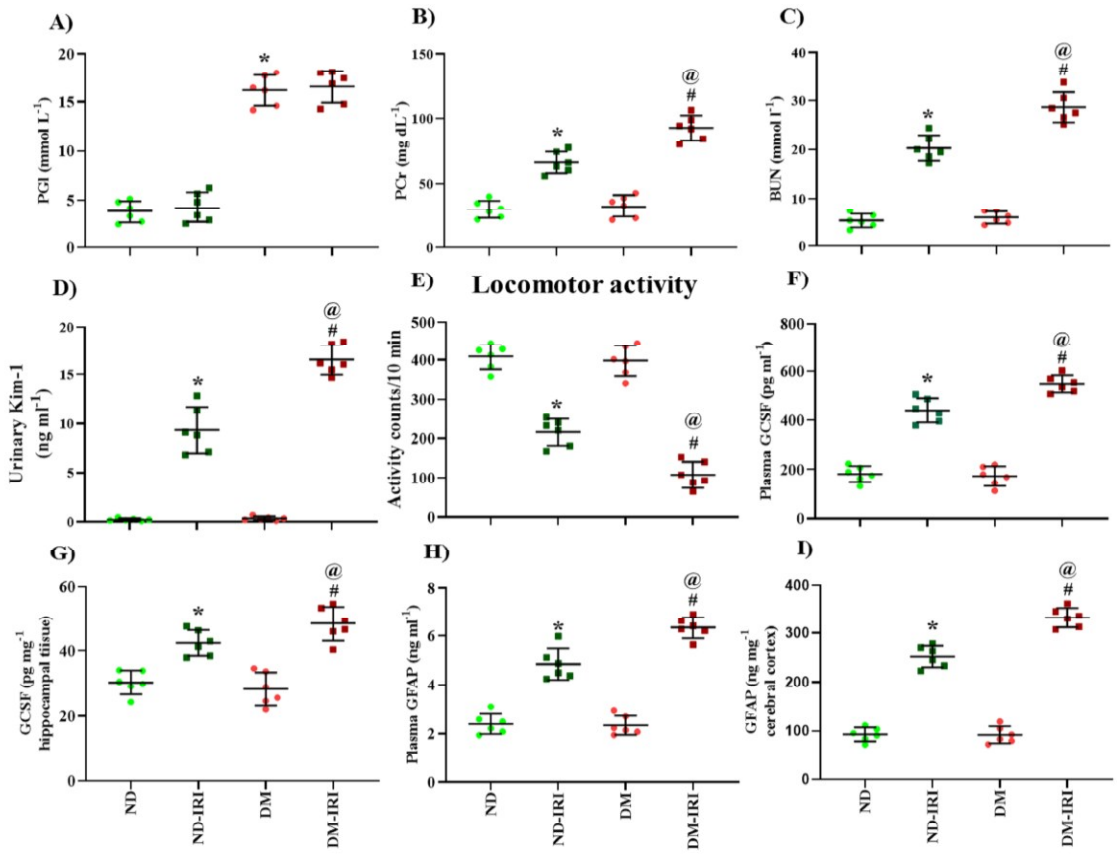

Figure 5.19 Evaluation of plasma and urine biochemistry, locomotor activity, and brain-specific GCSF and GFAP protein levels under IRI.

A-C: Estimation of renal parameters in plasma e.g. plasma glucose (PGL) (A), creatinine (PCr) (B), and blood urea nitrogen (BUN) (C), likewise, scattered plot of urinary kidney injury molecule-1 (Kim-1) (D). F-I: Scattered plots displayed plasma (F) and hippocampal levels of granulocyte-colony stimulating factor (GCSF) (G); plasma (H) and cerebral cortex levels of glial fibrillary acidic protein (GFAP) (I). All the values are represented as mean ± S.D. (n=6). For statistical comparison, one-way ANOVA with Tukey's multiple comparison test was used where (*) P < 0.05 vs ND; (#) P < 0.05 vs DM; (@) P < 0.05 vs ND-IRI.

5.4.3. AT2R and ACE2 activation accentuated renal functions in diabetic and non-diabetic rats upon ischemic renal injury.

We adjured to check the role of RAS depressor arms' regulations on the brain after IRI. We treated ND-IRI and DM-IRI rats with AT2R agonist (C21, 0.3 mg/kg/day, *i.p.*) and ACE2 activator (Dize, 5 mg/kg/day, *p.o.*), either alone as monotherapy or together as combination therapy. Plasma biochemical parameters revealed that none of the therapies had any effect on increased plasma glucose levels in the DM group ***(Figure 5.20 A)***. ND-

IRI and DM-IRI rats' receiving C21 and Dize combination therapy significantly reduced BUN levels, while both the monotherapies had no effect on BUN levels when compared to respective controls ***(Figure 5.20 B)***. Both monotherapies and combination therapy showed a significant reduction in PCr levels when compared to ND-IRI and DM-IRI rats. Interestingly, the combination therapy exhibited lower levels of PCr compared to both monotherapies in ND and DM conditions ***(Figure 5.20 C)***. Moreover, in ND-IRI rats, combination therapy has significantly reduced PCr levels compared to DM-IRI rats. In the ND group, the increased urinary Kim-1 level was significantly decreased by C21 and Dize monotherapies and combination therapy ***(Figure 5.20 D)***. In the DM group, only combination therapy had an effect on decreasing urinary Kim-1 levels compared to DM-IRI and both monotherapies ***(Figure 5.20 D)***. Moreover, ND-IRI+CD rats have significantly lowered the urinary Kim-1 levels compared to DM-IRI+CD rats.

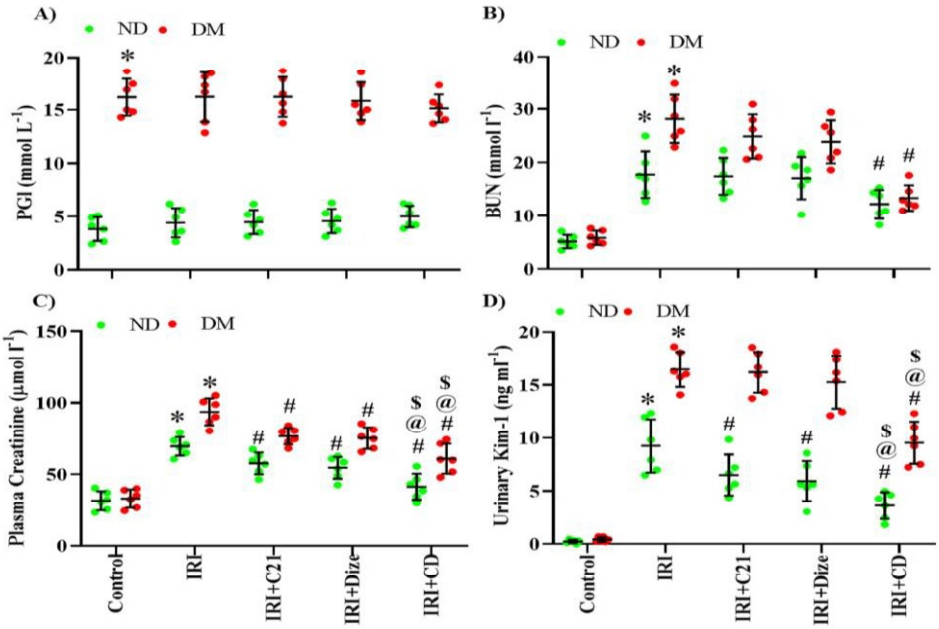

Figure 5.20 Effect of AT2R and ACE2 activation on plasma and urine biochemistry.

A-D: Representative scattered plots of plasma glucose (PGl) (A), creatinine (PCr) (B), blood urea nitrogen (BUN) (C) and urinary kidney injury molecule-1 (Kim-1) (D). Data are represented as mean ± S.D. (n=6). For statistical comparison, two-way ANOVA with Tukey's multiple comparison test was used where (*) P < 0.05 vs control; (#) P < 0.05 vs IRI; (@) P < 0.05 vs IRI-C21; ($) P < 0.05 vs IRI-Dize.

5.4.4. AT2R and ACE2 activation improved cognitive functions and diminished oxidative stress.

As compared to ND-IRI rats, DM-IRI rats had a significant decrease in locomotor activity ***(Figure 5.21 A)***. Interestingly, concomitant activation of AT2R and ACE2 had improved the activity counts in ND-IRI and DM-IRI rats, while ND-IRI rats showed marked recovery as compared to DM-IRI rats. Neither of the monotherapies had improved the locomotor-cognitive function in ND-IRI and DM-IRI rats ***(Figure 5.21 A)***.

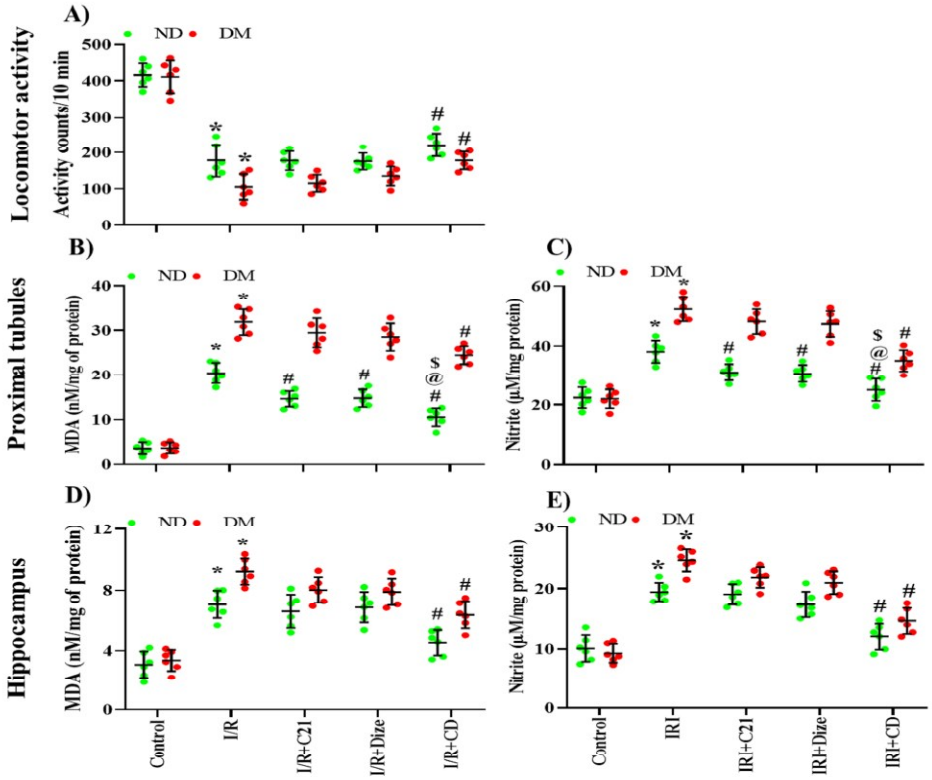

Figure 5.21 Effect of AT2R and ACE2 activation on locomotor activity, and proximal tubular and hippocampal oxidative stress.

A-B: Estimation of oxidative stress markers e.g. malondialdehyde (MDA) (A), nitrite (B) levels in the isolated proximal tubular fraction from rat kidneys (n=6). C-D: Estimation of oxidative stress markers; malondialdehyde (MDA) (A), nitrite (B) levels in hippocampal homogenate obtained from rat brain tissue (n=6). Scattered plot (E) of locomotor activity which was evaluated by the times breaking laser beam during the test. Data are represented as mean ± S.D. from three independent experiments. Two-way ANOVA with Tukey's multiple comparison test for statistical comparison. (*) P < 0.05 vs control; (#) P < 0.05 vs IRI; (@) P < 0.05 vs IRI-C21; ($) P < 0.05 vs IRI-Dize.

Further, we tested MDA and nitrite levels to determine whether hyperglycemia aggravated IRI-associated brain functional abnormalities are linked with brain oxidative stress levels. In proximal tubules, DM-IRI rats showed higher MDA and nitrite levels as compared to ND-IRI rats ***(Figure 5.21 B, C)***. In the ND group, C21 and Dize monotherapies have reduced the MDA and nitrite levels compared to ND-IRI rats. However, combination therapy significantly reduced the MDA and nitrite levels compared to C21 and Dize monotherapies ***(Figure 5.21 B, C)***. In the DM group, C21 and Dize monotherapies had no effect on MDA and nitrite levels, but combination therapy significantly lessened MDA and nitrite levels compared to DM-IRI rats ***(Figure 5.21 B, C)***. In hippocampal tissue, DM-IRI rats showed a significant elevation of MDA and nitrite levels compared to ND-IRI rats ***(Figure 5.21 D, E)***. Neither of the monotherapies lowered the hippocampal MDA and nitrite levels ***(Figure 5.21 D, E)***. However, the combination therapy significantly attenuated the MDA and nitrite levels as compared to ND-IRI and DM-IRI rats ***(Figure 5.21 D, E)***.

5.4.5. AT2R and ACE2 activation suppressed pyknotic neurons in the hippocampal CA1 region of diabetic and non-diabetic rats after ischemic renal injury.

Light microscopic data of H and E stained brain sections showed healthy neurons in the CA1 region of the hippocampus in ND and DM rats ***(Figure 5.22 A)***. Healthy neurons seemed robust, spherical, or slightly oval nucleus with clear visible cytoplasm as indicated by green arrows. However, the ND-IRI and DM-IRI groups showed disorganization and cell loss in the CA1 region as indicated by red arrows ***(Figure 5.22 A, B)***. The pyknotic cell count was more prominent with DM-IRI group in comparison to ND-IRI group (***Figure 5.22 B***). The size of pyramidal cells was substantially shrunken with darkened nuclei. Remarkably, there was a reduction in the pyknotic neurons and apoptosis, and preservation of pyramidal cells following treatment with C21 and Dize combination therapy compared to ND-IRI and DM-IRI groups ***(Figure 5.22 A, B)***. In the ND group, combination therapy significantly reduced pyknotic cells count compared to the DM group with combination therapy. In contrast, both monotherapies were unable to produce a significant reduction in pyknotic cells counts compared to ND-IRI and DM-IRI rats ***(Figure 5.22 A, B)***.

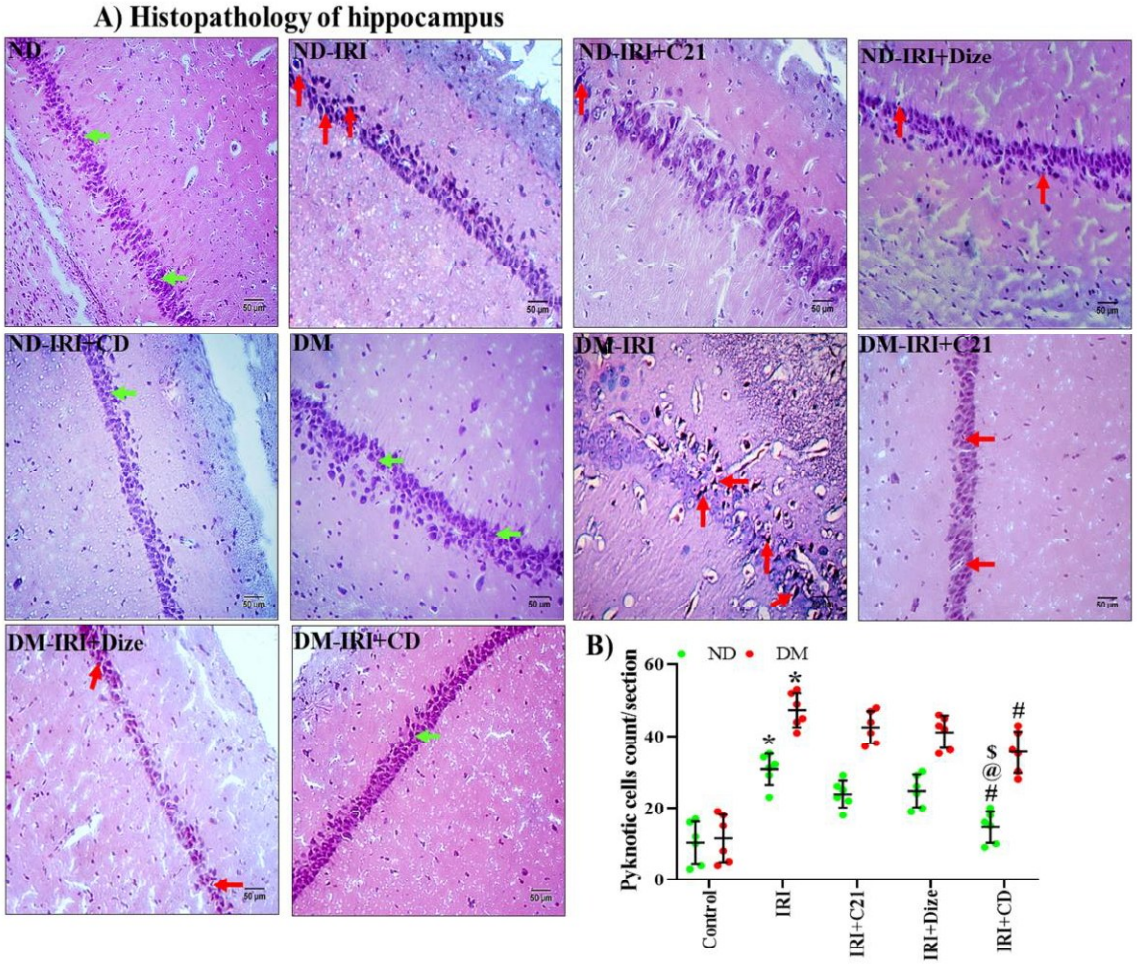

Figure 5.22 Effect of AT2R and ACE2 activation on pyknotic neurons in the hippocampus of the brain.

The brain samples from each group were collected at 24 h after surgery and were processed for histological examination by H and E staining. Representative images of brain sections magnifying the CA1 region of the hippocampus (original magnification 400x and scale bar- 50 µm). At least 4-5 images from each stained brain section and a total of six different brains per group were observed by a blinded observer for healthy (Green arrow) and pyknotic neuronal cells (Red arrow) (A). The pyknotic cell count was analyzed semi-quantitatively (B). Data are represented as mean ± S.D. Two-way ANOVA with Tukey's multiple comparison test was applied for statistical comparison. (*) P < 0.05 vs control; (#) P < 0.05 vs IRI; (@) P < 0.05 vs IRI-C21; ($) P < 0.05 vs IRI-Dize.

5.4.6. AT2R and ACE2 activation curbed systemic and brain soluble inflammatory mediator-GFAP in diabetic and non-diabetic rats upon ischemic renal injury.

Regarding GCSF, DM-IRI rats showed a significant increase in its plasma and hippocampal GCSF levels as compared to ND-IRI rats ***(Figure 5.23 A, B)***. Neither monotherapies nor combination therapies have observed to persuade a significant difference in the plasma and hippocampal GCSF protein levels compared with ND-IRI and DM-IRI rats ***(Figure 5.23 A, B)***. In plasma and cerebral cortex homogenate samples, DM-IRI rats showed a significant increase in GFAP protein levels compared to ND-IRI rats ***(Figure 5.23 C, D)***. C21 and Dize monotherapies showed no effect on GFAP protein levels compared to ND-IRI and DM-IRI rats. In ND and DM studies, combination therapy significantly lowers the GFAP levels as compared to IRI and monotherapies groups ***(Figure 5.23 C, D)***. In combination therapy, DM-IRI rats showed less reduction GFAP levels compared to ND-IRI rats in plasma and cerebral cortex (***Figure 5.23 C, D***) samples.

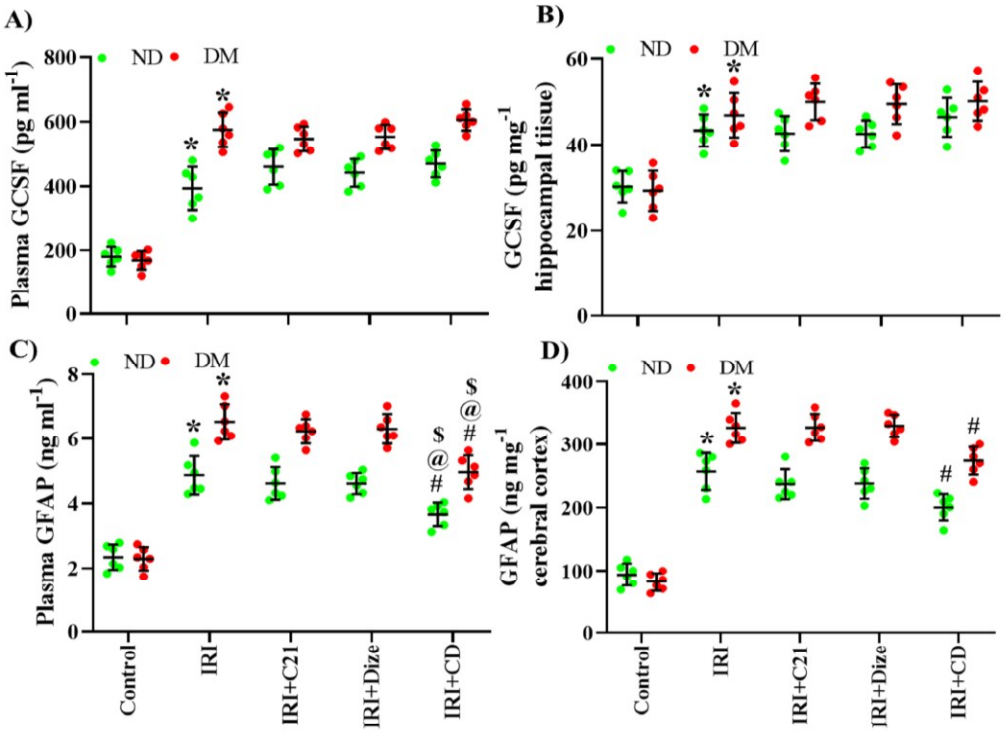

Figure 5.23 Effect of C21 and Dize on systemic, hippocampal, and cerebral cortex levels of GCSF and GFAP.

A-B: Protein levels of GCSF in plasma (A) and hippocampal tissue (B); C-D: Protein levels of GFAP in plasma (C) and cerebral cortex (D) as measured by ELISA (n=6). Data are represented as mean ± S.D. Two-way ANOVA with Tukey's multiple comparison test was applied for statistical

comparison. (*) P < 0.05 vs control; (#) P < 0.05 vs IRI; (@) P < 0.05 vs IRI-C21; ($) P < 0.05 vs IRI-Dize.

5.4.7. AT2R and ACE2 activation attenuated TNF-alpha expression in the hippocampal CA1 region after ischemic renal injury.

We observed that DM-IRI and ND-IRI rats presented marked elevation of TNF-α expressions in the CA1 hippocampal region compared to respective controls ***(Figure 5.24 A, B)***. Here, DM-IRI group showed higher TNF-α expressions compared to ND-IRI group (***Figure 5.24 B***). In ND and DM studies, C21 and Dize combination treatment had significantly reduced the TNF-α expressions as compared to IRI and monotherapies group. In combination therapy, ND-IRI rats showed a marked reduction in TNF-α expressions compared to DM-IRI rats (***Figure 5.24 B***).

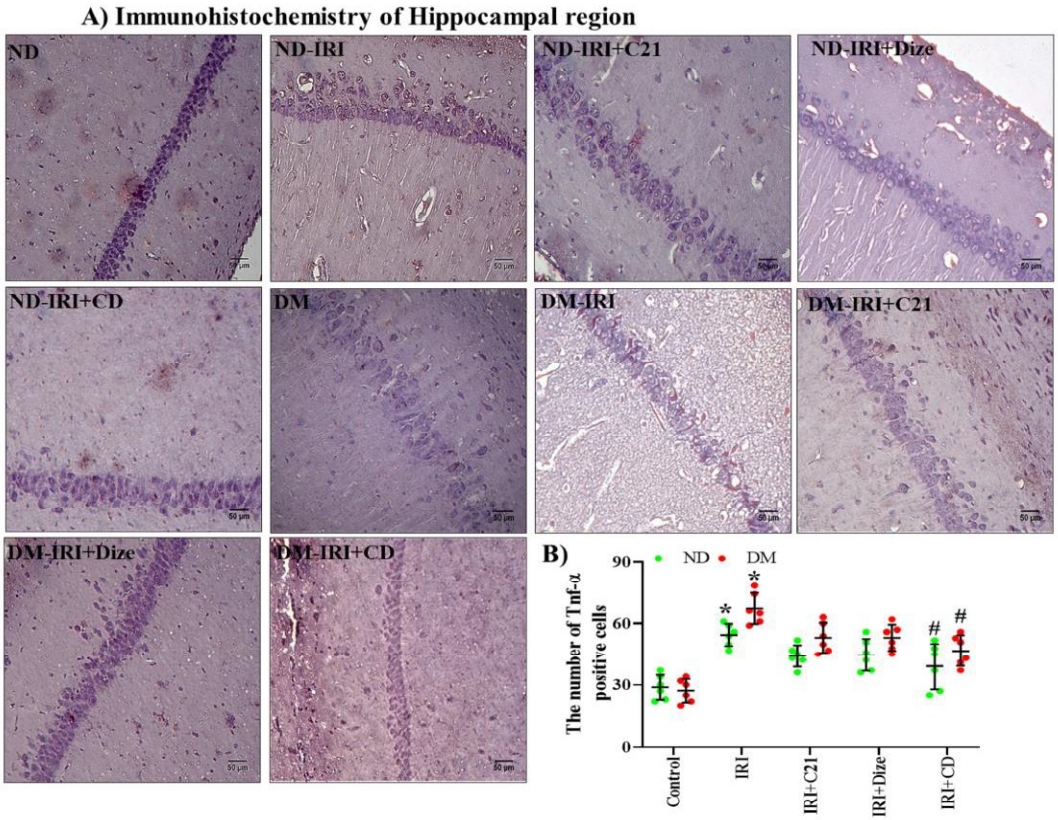

Figure 5.24 Immunohistochemistry for TNF-α in the CA1 region of the hippocampus.

A: Representative images of IHC staining for TNF-α in the CA1 region of the hippocampus (original magnification 400× and scale bar 50μm). Around 4-5 sections from each stained brain microscopy slide and a total of six different brain slides per group were seen under a microscope and images were captured. B: Semi-quantitative analysis of all the images via ImageJ (color

deconvolution plugin was utilized for analysis) for calculating the DAB-positive area. All Data are represented as mean ± S.D. Two-way ANOVA with Tukey's multiple comparison test was used for statistical comparison. (*) P < 0.05 vs control; (#) P < 0.05 vs IRI; (@) P < 0.05 vs IRI-C21; ($) P < 0.05 vs IRI-Dize.

5.4.8. AT2R and ACE2 activation modulated RAS components in the proximal tubular cells of diabetic and non-diabetic rats upon ischemic renal injury.

We have checked the proximal tubular levels of the pressor arm and the depressor arm of RAS. In ***figure 5.25***, the ACE and Ang II levels of ND-IRI and DM-IRI were significantly greater than their respective controls. The DM-IRI rats showed a significant increase in ACE and Ang II levels compared to ND-IRI rats (***Figure 5.25 A, C***). C21 and Dize alone and in combination did not reduce the ACE levels. However, combination therapy of C21 and Dize has markedly reduced the Ang II levels as compared to in ND/DM-IRI and monotherapies groups ***(Figure 5.25 C)***. Here, combination treatment in DM-IRI rats showed a comparatively lesser reduction of Ang II levels as compared to ND-IRI rats. Further, depressor arm components: ACE2 ***(Figure 5.25 B)*** and Ang (1-7) ***(Figure 5.25 D)*** levels were significantly reduced in proximal tubules of ND-IRI and DM-IRI groups compared to their respective controls. ND-IRI rats showed less significant reduction in ACE2 and Ang (1-7) levels compared to DM-IRI rats (***Figure 5.25 B, D***). Among monotherapies, only Dize treatment increased ACE2 ***(Figure 5.25 B)*** and Ang (1-7) ***(Figure 5.25 D)*** levels compared to ND-IRI and DM-IRI rats. Moreover, combination therapy significantly increased ACE2 ***(Figure 5.25 B)*** and Ang (1-7) levels ***(Figure 5.25 D)*** compared to ND/DM-IRI and monotherapies groups.

In ***figure 5.25 E***, urinary AGT levels were significantly elevated in ND-IRI and DM-IRI rats in comparison to ND and DM rats. Though, DM-IRI rats showed higher urinary AGT levels compared to ND-IRI rats (***Figure 5.25 E***). Combination therapy has significantly reduced urinary AGT levels compared to ND-IRI and DM-IRI rats. However, combination treatment in DM-IRI rats showed a comparatively lesser reduction of urinary AGT levels than the ND group of combination therapy.

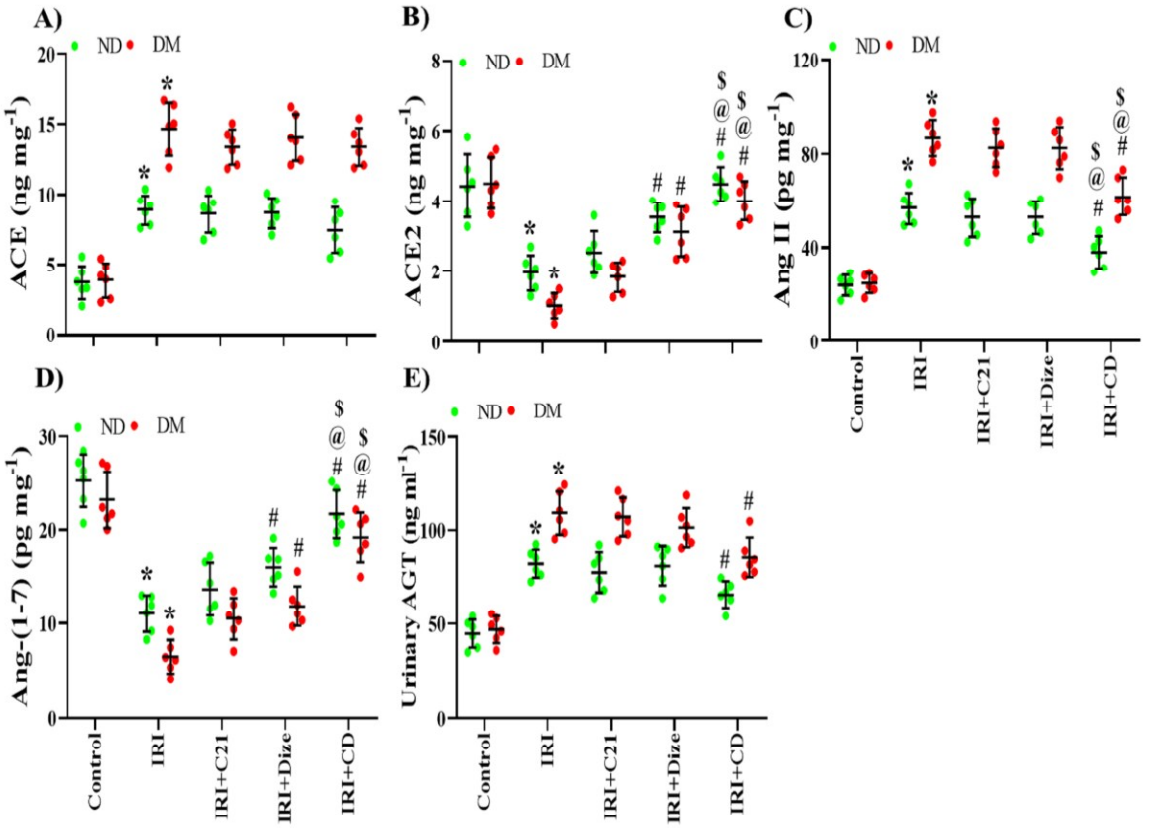

Figure 5.25 AT2R and ACE2 activation modulate protein levels of pressor and depressor components of RAS in proximal tubules.

A-D: Protein levels of ACE, ACE2, Ang II, and Ang (1-7) in isolated proximal tubules, and urinary AGT (E) was measured by ELISA (n=6). Data are represented as mean ± S.D. Two-way ANOVA with Tukey's multiple comparison test was applied for statistical comparison. (*) P < 0.05 vs control; (#) P < 0.05 vs IRI; (@) P < 0.05 vs IRI-C21; ($) P < 0.05 vs IRI-Dize.

5.4.9. AT2R and ACE2 activation improved hippocampal depressor arm and suppressed pressor arm components of diabetic and non-diabetic rats upon ischemic renal injury.

In AKI, neurons get activated in stress-sensitive brain regions including the hippocampus (Palkovits et al., 2009). In ND-IRI and DM-IRI rats, the hippocampal levels of Ang II ***(Figure 5.26 A)*** and Ang-(1-7) ***(Figure 5.26 B)*** were significantly increased and decreased, respectively, as compared to ND and DM rats. For hippocampal Ang II levels, DM-IRI rats showed higher Ang II levels as compared to ND-IRI rats. After combination therapy, ND-IRI rats showed a significant reduction in Ang II levels compared to DM-IRI rats. For hippocampal Ang (1-7) levels, ND-IRI rats showed lesser reduction in Ang (1-7) levels as

compared to DM-IRI rats. Among monotherapies, only Dize therapy has increased the Ang (1-7) levels as compared to ND-IRI and DM-IRI rats. The combination therapy with C21 and Dize results in significant increased Ang (1-7) levels as compared to ND/DM-IRI and both monotherapies groups ***(Figure 5.26 A, B)***. IRI has significantly increased the hippocampal *At1r* mRNA expressions compared to ND and DM rats ***(Figure 5.26 C)***. DM-IRI rats showed significantly elevated *At1r* mRNA expressions in comparison to ND-IRI rats. Here, neither monotherapies nor combination therapy normalized the *At1r* mRNA expression compared to ND-IRI and DM-IRI rats ***(Figure 5.26 C)***.

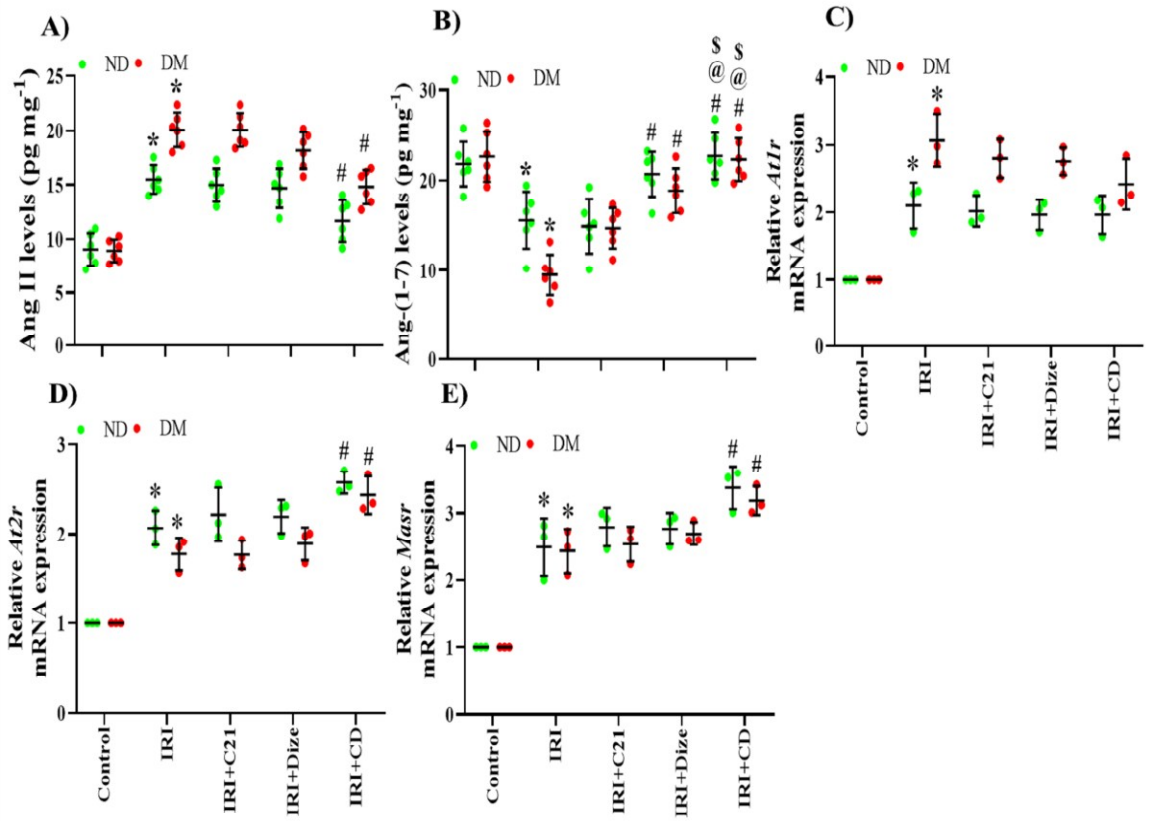

Figure 5.26 Effect of C21, Dize, and their combination therapy on protein and mRNA expressions of RAS components in hippocampal tissue.

A-B: Protein expression of Ang II and Ang (1-7) in hippocampal tissue homogenate was assessed by ELISA (n=6). C-D: mRNA expressions of At1r, At2r, and Masr were checked by qRT-PCR in the brain hippocampus. 18s rRNA expression was used as an internal control. Data are represented as mean ± S.D. from three independent experiments. Two-way ANOVA with Tukey's multiple comparison test was utilized for statistical comparison. (*) P < 0.05 vs control; (#) P < 0.05 vs IRI; (@) P < 0.05 vs IRI-C21; ($) P < 0.05 vs IRI-Dize.

On the other hand, the key receptors of the depressor arm of RAS i.e. *At2r, Masr* mRNA expressions got elevated in ND-IRI and DM-IRI rats compared to ND and DM rats ***(Figure 5.26 D, E)***. Additionally, the combination treatment significantly raised the *At2r* and *Masr* mRNA expressions as compared to ND-IRI and DM-IRI rats ***(Figure 5.26 D, E)***. However, none of the monotherapies upregulated the *At2r* and *Masr* mRNA expressions.

5.4.10. Effect of AT2R and ACE2 activation on cardiac and hepatic functional parameters.

After surgery, IRI showed no significant changes in SBP in ND and DM rats. Either alone or combination therapy had not exerted any alteration in SBP of ND/DM-IRI rats ***(Table 5.3)***. Further, cardiac injury markers i.e., CK-MB and LDH, and hepatic biomarkers i.e., ALT and AST were significantly elevated in ND and DM rats underwent IRI ***(Table 5.3)***. However, DM-IRI rats showed significant elevation ($P < 0.05$) in cardiac and hepatic injury markers compared to ND-IRI rats. Combination therapy of C21 and Dize has markedly reduced ($P < 0.05$) the plasma levels of CK-MB, LDH, ALT, and AST compared to IRI groups of ND and DM rats. However, monotherapies have reduced the plasma levels of CK-MB, LDH, ALT and AST in ND/DM IRI rats, but not significantly.

Table 5.3 Effect of AT2R and ACE2 activation on cardiac and liver-specific parameters.

Groups	SBP (mmHg)	CK-MB (IU/L)	LDH (IU/L)	ALT (IU/L)	AST (IU/L)
ND	105 ± 4.7	307.4 ± 38.2	273.3 ± 33.1	27.28 ± 2.4	23.84 ± 5.8
ND-IRI	104 ± 5.2	802.7 ± 52.4*	982.4 ± 48.4*	64.23 ± 3.7*	54. 24 ± 4.9*
ND-IRI+C21	105 ± 8.4	751.2 ± 42.5	832.9 ± 75.2	52.13 ± 4.6	50.32 ± 8.3
ND-IRI+Dize	106 ± 6.9	724.7 ± 55.3	743.1 ± 63.9	48.53 ± 5.2	47.96 ± 6.8
ND-IRI+CD	107 ± 5.5	461.9 ± 34.8$^{@}$	412.4 ± 43.1$^{@}$	32.94 ± 3.7$^{@}$	36.24 ± 4.2$^{@}$
DM	105 ± 4.7	312.3 ± 53.5	280.2 ± 37.2	28.01 ± 1.9	24.13 ± 4.5

DM- IRI	106 ± 3.9	1220.8 ± 93.7$^{\#,@}$	1343.6 ± 78.8 $^{\#,@}$	84.94 ± 4.1 $^{\#,@}$	60. 65 ± 3.9$^{\#,@}$
DM-IRI+C21	104 ± 3.8	1038.2 ± 72.9	1047.9 ± 69.2	70.29 ± 3.8	55.87 ± 4.1
DM-IRI+Dize	106 ± 4.5	1091.4 ± 87.2	1098.7 ± 84.7	67.38 ± 5.7	56.12 ± 4.6
DM-IRI+CD	109 ± 6.1	726.7 ± 56.2$^{\$}$	628.8 ± 81.3$^{\$}$	43.92 ± 3.2$^{\$}$	43.56 ± 3.5$^{\$}$

SBP- *Systolic blood pressure,* ***CK-MB-*** *Creatine kinase-MB,* ***LDH-*** *Lactate dehydrogenase,* ***AST-*** *Aspartate aminotransferase,* ***ALT-*** *Alanine transaminase.* ***Note:*** *Each data is represented as mean ± SD (n=6). (*) p < 0.05 vs ND; (@) p < 0.05 vs ND-IRI; (#) p < 0.05 vs DM; ($) p < 0.05 vs DM-IRI.*

5.4.11. Effect of AT2R and ACE2 activation on oxidative/ antioxidant status

Oxidative stress is one of the major inflammation triggering factors for the progression of AKI and its associated distant organ dysfunction (Kanagasundaram, 2015). In heart and liver tissue homogenates, oxidative stress was found to be elevated significantly ($P < 0.05$) in ND/DM IRI rats, owing to an increase in MDA levels ***(Figure 5.27 A, E)*** and MPO activity ***(Figure 5.27 B, F)***. However, only combination therapy of C21 and Dize has effectively reduced their levels ($P < 0.05$) in ND/DM IRI rats as compared to their respective controls ***(Figure 5.27 A-B, E-F)***. On the other hand, the anti-oxidant defense mechanism gets hampered by IRI, observed by reduced ($P < 0.05$) GSH levels and catalase activity in heart and liver tissues of ND/DM rats ***(Figure 5.27 C-D, G-H)***. Interestingly, the combination therapy has effectively normalized the GSH and catalase activity in heart and liver tissues. Moreover, both monotherapies showed no effect on ND, and DM rats underwent IRI.

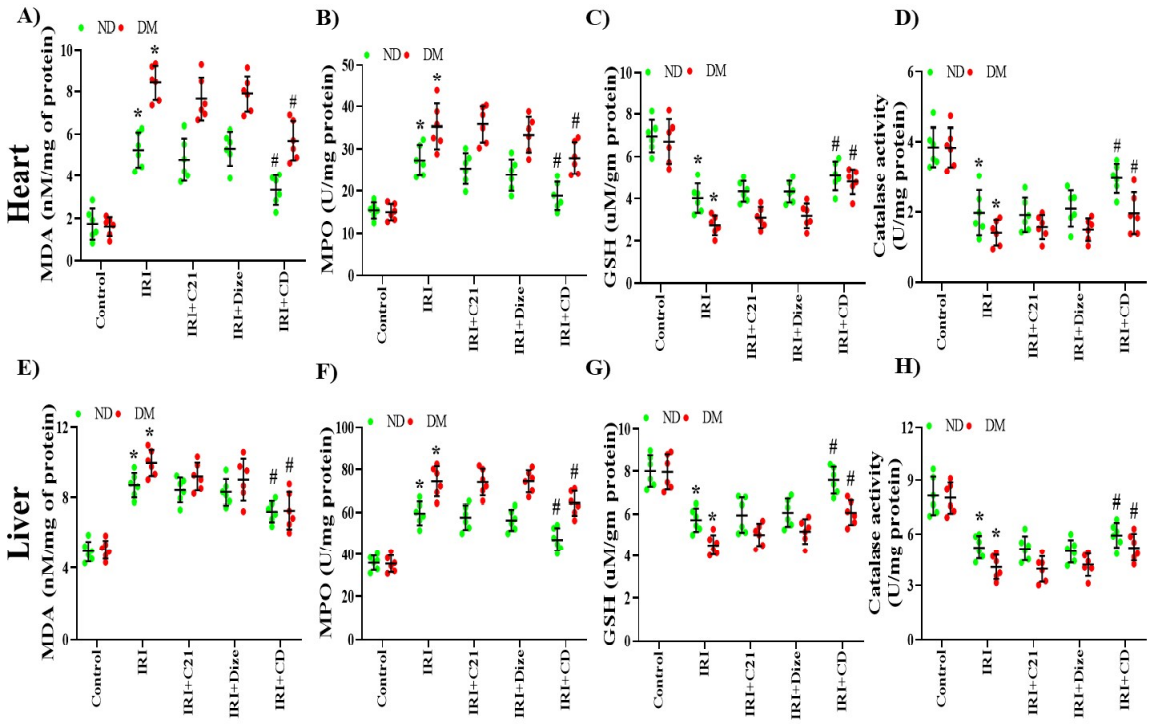

Figure 5.27 Effect of AT2R and ACE2 activation on heart and liver oxidative stress.

A-H: Estimation of oxidative stress markers e.g. malondialdehyde (MDA) levels (A, E), Myeloperoxidase (MPO) activity (B, F), glutathione (GSH) levels (C, G), catalase activity (D, H) in isolated heart and liver tissues (n=6). Data are represented as mean ± S.D. from three independent experiments. Two-way ANOVA with Tukey's multiple comparison test for statistical comparison. (*) $p < 0.05$ vs Control; (#) $p < 0.05$ vs IRI.

5.4.12. Histopathological findings

In the current study, histopathological changes in hepatic and cardiac tissue samples obtained from all groups were evaluated using microscopy. The cardiac histological architecture in tissue from ND and DM rats appeared as regularly arranged cardiac myofibers having several cardiac myocytes comprising mainly of single, ovoid, and centrally located nuclei ***(Figure 5.28 A, F)***. After IRI, histopathology revealed severe myocardial degenerative changes, which were identified by disarrayed cardiac muscle fibers (shown by the yellow arrow) ***(Figure 5.28 B, G)***. Meanwhile, IRI rats with combination therapy exhibited mild myocardial degenerative changes ***(Figure 5.28 E, J)***.

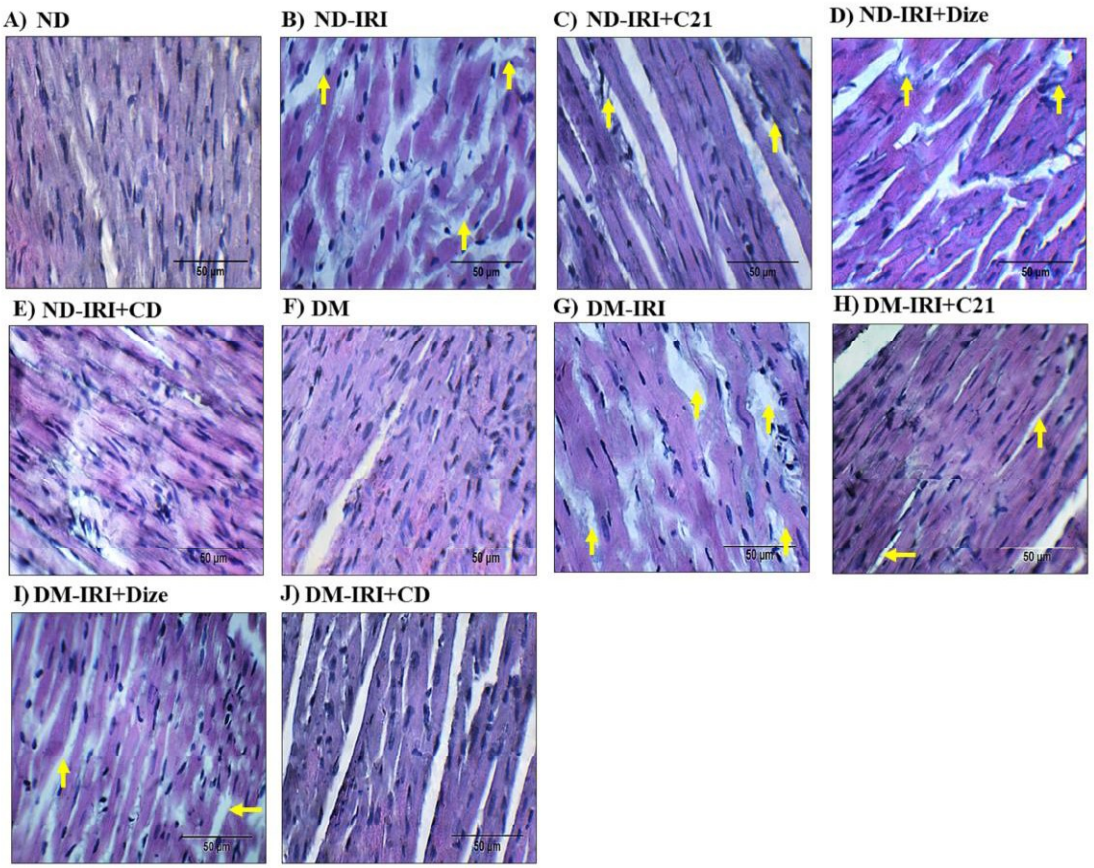

Figure 5.28 Effect of AT2R and ACE2 activation on histopathological findings in the heart.

The heart samples from each group were collected after reperfusion and were processed for histological examination by H and E staining. A-J: Representative images of heart sections magnifying cardiac muscle fibers (original magnification 100x and scale bar- 50 µm). 4-5 images from each stained heart section and a total of six different heart per group were observed by a blinded observer for healthy as well as disarrayed cardiac muscle fibers (Yellow arrow) (A).

The hepatic histological architecture in tissue sections from ND and DM rats showed normal, lobular structure with finely arranged hepatic cords embracing large polyhedral cells with spherical vesicular nuclei. In addition, Kupffer cells and hepatic sinusoids were located in-between the radiating hepatic cords ***(Figure 5.29 A, F)***. After IRI, ND/DM rats were showed sinusoidal dilatation and vacuolization of hepatocytes along with leukocytes infiltration (shown by the yellow arrow), pyknotic nuclei, and Kupffer cell proliferation ***(Figure 5.29 B, G)***. Interestingly, combination therapy of C21 and Dize has markedly reduced the histopathological alterations such as reduced vacuolization of hepatocytes and

decreased hepatocellular degeneration ***(Figure 5.29 E, J)***. On the other hand, both monotherapies have mildly reduced the vacuolization of hepatocytes ***(Figure 5.29 C-D, H-I)***.

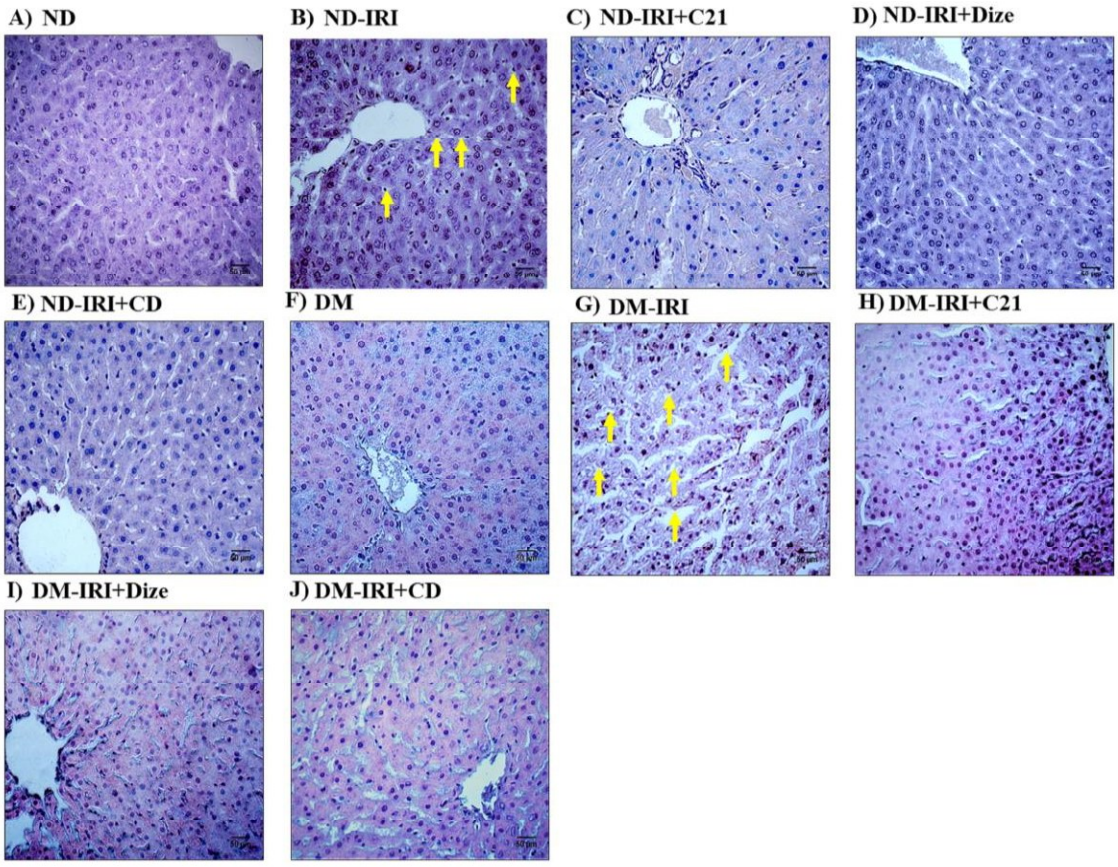

Figure 5.29 Effect of AT2R and ACE2 activation on histopathological findings in the liver.

The liver samples from each group were collected after reperfusion and were processed for histological examination by H and E staining. A-J: Representative images of liver sections (original magnification 100x and scale bar- 50 μm). 4-5 images from each stained liver section and a total of six different liver per group were observed by a blinded observer. Sinusoidal dilatation and vacuolization of hepatocytes along with leukocytes infiltration (shown by the yellow arrow).

5.4.13. Effect of AT2R and ACE2 activation on TNF-α mediated cardiac and hepatic inflammation.

We have checked the immunohistochemical TNF-α expressions to evaluate whether the C21 and Dize reduced the IRI-induced cardio-hepatic inflammation. In cardiac tissue

sections, we found that IRI in ND and DM rats increased ($P < 0.05$) the TNF-α expressions as compared to their respective controls ***(Figure 5.30 A, F)***. As compared to ND-IRI group, DM-IRI group showed significant elevation ($P < 0.05$) in the TNF-α expression. Interestingly, simultaneous activation of AT2R and ACE2 by combination therapy of C21 and Dize had significantly decreased ($P < 0.05$) the TNF-α expressions in comparison to ND and DM rats underwent IRI ***(Figure 5.30 B, G)***. Moreover, both monotherapies had decreased the TNF-α expressions in ND/DM-IRI rats, followed by significant reduction by combination therapy ***(Figure 5.30 K)***.

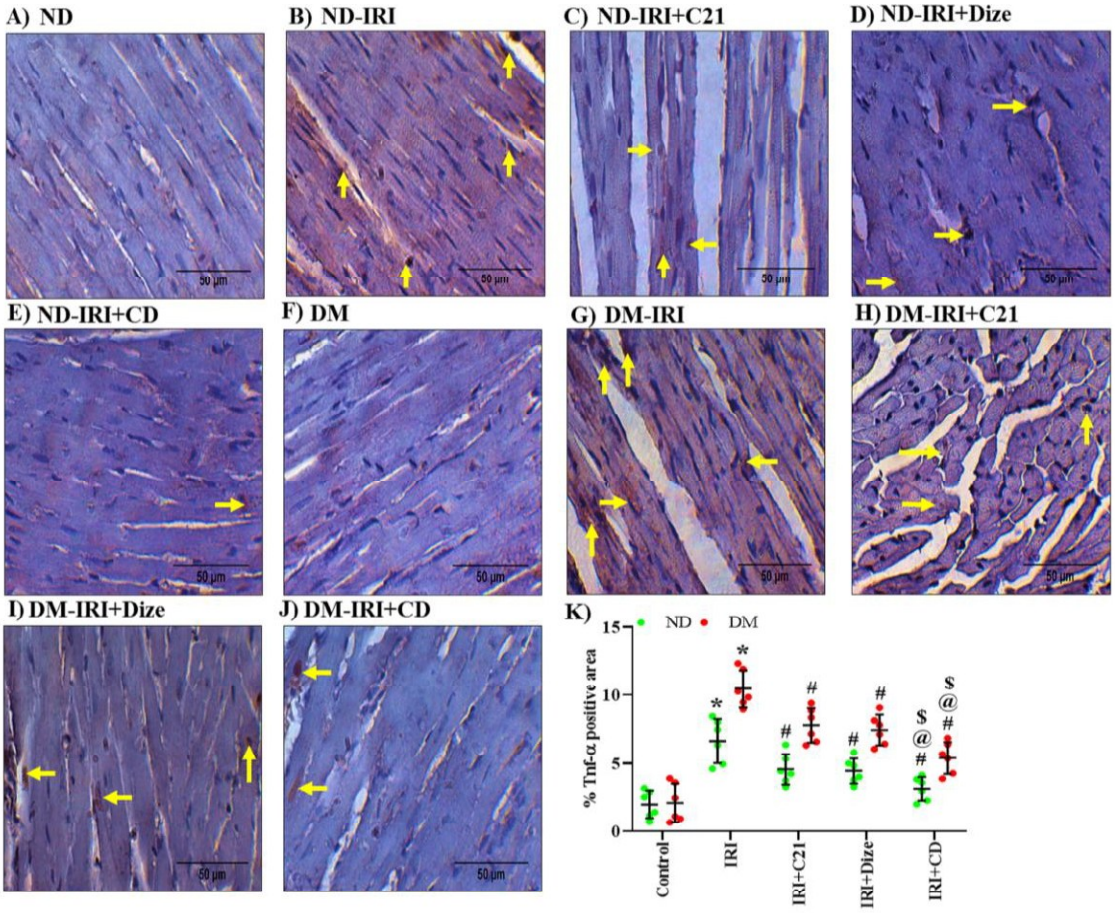

Figure 5.30 Effect of AT2R and ACE2 activation on TNF-α expression in the heart.

A-J: Representative images of IHC staining for TNF-α in the heart (original magnification 100x and scale bar 50µm). Around 4-5 sections from each stained heart microscopy slide and a total of six different heart slides per group were seen under a microscope and images were captured. K: Semi-quantitative analysis of all the images via ImageJ (color deconvolution plugin was utilized for analysis) for calculating the DAB-positive area. All Data are represented as mean ± S.D. Two-

way ANOVA with Tukey's multiple comparison test was used for statistical comparison. (*) p < 0.05 vs Control; (#) p < 0.05 vs IRI; (@) p < 0.05 vs IRI-C21; ($) p < 0.05 vs IRI-Dize.

In hepatic tissue sections, we found that a drastic increase in inflammation, as demonstrated by a multi-fold increase ($P < 0.05$) in TNF-α expressions in IRI groups of ND and DM rats ***(Figure 5.31 B, G)***. TNF-α mediated inflammation was significantly controlled ($P < 0.05$) by the combination treatment as compared to their respective control groups ***(Figure 5.31 E, J)***. Moreover, both the monotherapies also significantly suppress the hepatic TNF-α expressions as compared to ND/DM rats under IRI ***(Figure 5.31 K)***.

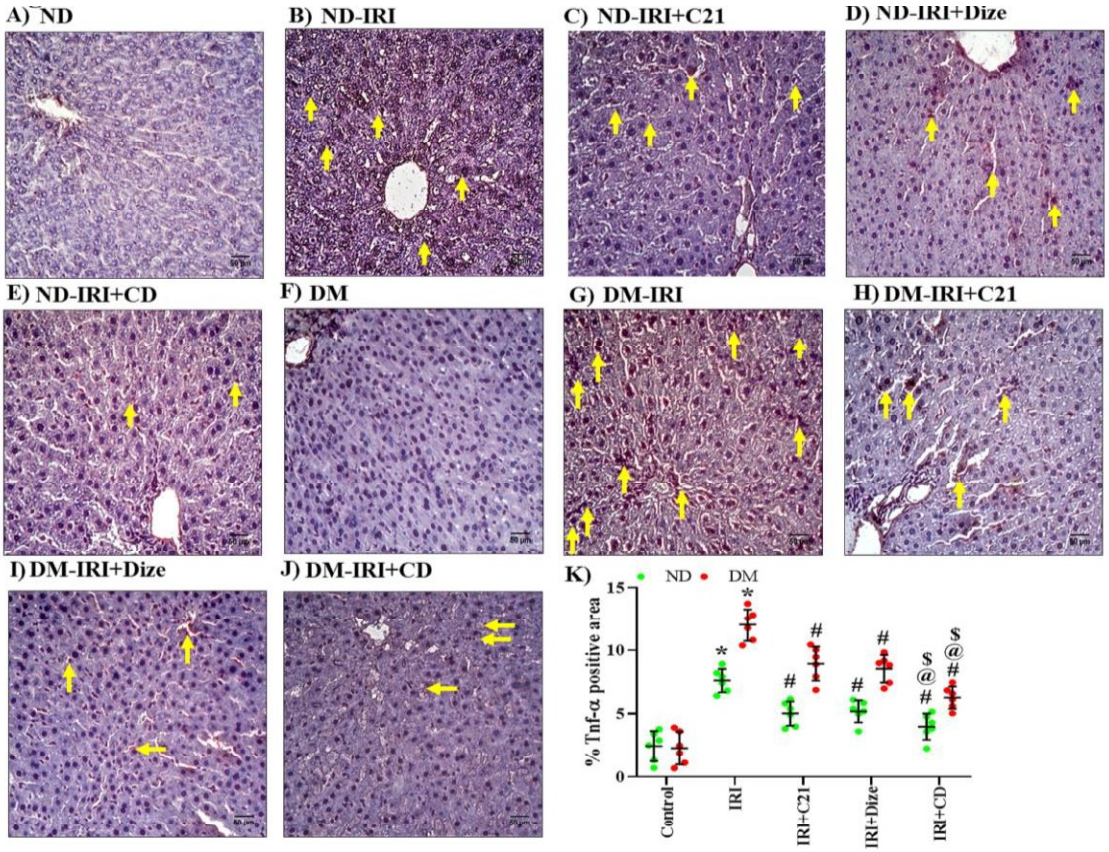

Figure 5.31 Effect of AT2R and ACE2 activation on TNF-α expression in the liver.

A-J: Representative images of IHC staining for TNF-α in the liver (original magnification 40x and scale bar 50μm). Around 4-5 sections from each stained liver microscopy slide and a total of six different liver slides per group were seen under a microscope and images were captured. B: Semi-quantitative analysis of all the images via ImageJ (color deconvolution plugin was utilized for analysis) for calculating the DAB-positive area. All Data are represented as mean ± S.D. Two-way ANOVA with Tukey's multiple comparison test was used for statistical comparison. (*) p < 0.05 vs Control; (#) p < 0.05 vs IRI; (@) p < 0.05 vs IRI-C21; ($) p < 0.05 vs IRI-Dize.

5.4.14. Effect of AT2R and ACE2 on systemic and cardio-hepatic depressor arm and pressor arm of RAS

In systemic circulation, heart, and liver tissues, we have checked the RAS specific enzymes i.e. ACE and ACE2. Here, IRI results in a significant increment ($P < 0.05$) in ACE levels compared to ND and DM rats ***(Figure 5.32 A-C).*** In plasma, ACE levels were found to be higher ($P < 0.05$) in DM rats compared to ND rats who underwent IRI. Interestingly, C21 and Dize combination therapy have significantly reduced the plasma, heart, and liver ACE levels when compared to ND/DM-IRI rats. However, none of the monotherapies was able to reduce ACE levels ***(Figure 5.32 A-C)***.

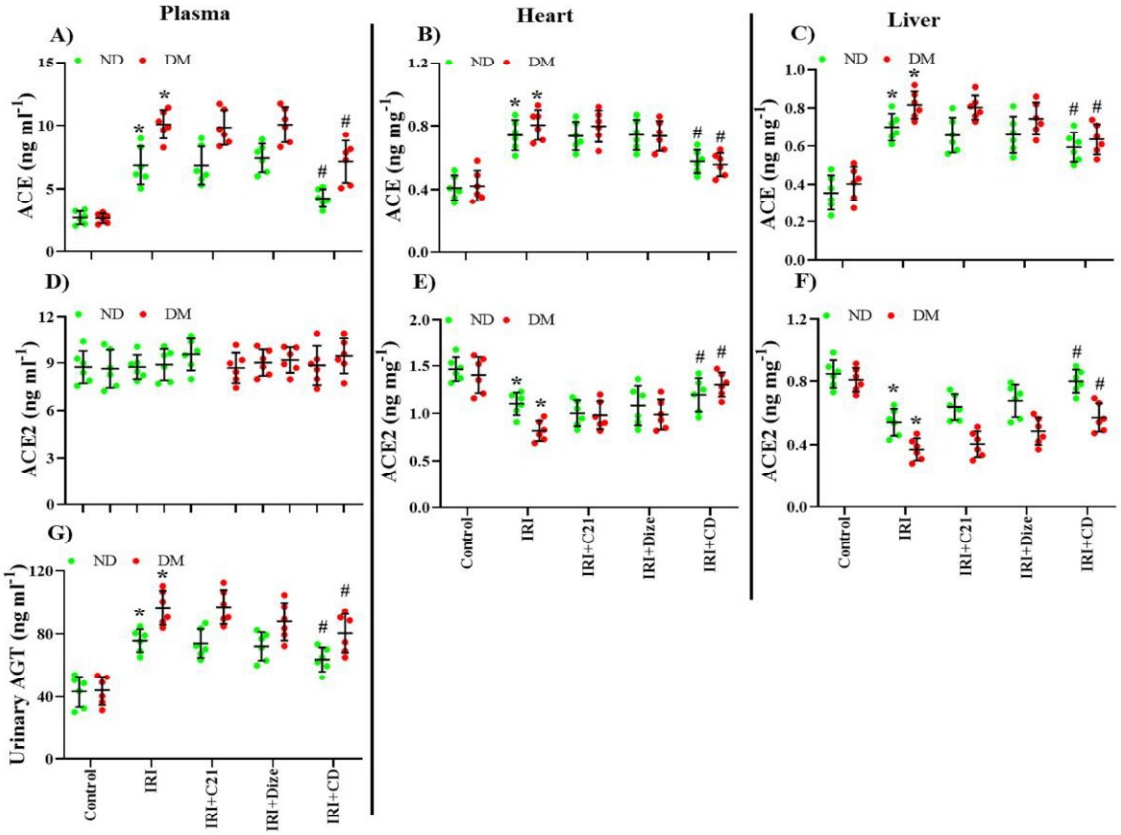

Figure 5.32 Effect of AT2R and ACE2 activation on protein levels of ACE, ACE2 in plasma, heart, and liver tissues along with urinary AGT.

A-F: Protein expression of ACE and ACE2 in plasma (A, D), heart (B, E), and liver (C, F), whereas protein expression of urinary AGT (G) was assessed by ELISA (n=6). Data are represented as mean ± S.D. from three independent experiments. Two-way ANOVA with Tukey's multiple comparison test was utilized for statistical comparison. (*) p < 0.05 vs Control; (#) p < 0.05 vs IRI.

On the other hand, IRI rats showed significant depletion of ACE2 levels in heart and liver tissues as compared to respective controls ***(Figure 5.32 E, F)***. However, combination therapy effectively normalized the ACE2 levels as compared to ND/DM-IRI rats ***(Figure 5.32 E, F)***. In contrast, systemic ACE2 levels remain unchanged across all the groups ***(Figure 5.32 D)***. We have also checked the levels of urinary AGT and found to get significantly elevated in ND and DM rats underwent IRI ***(Figure 5.32 G)***.

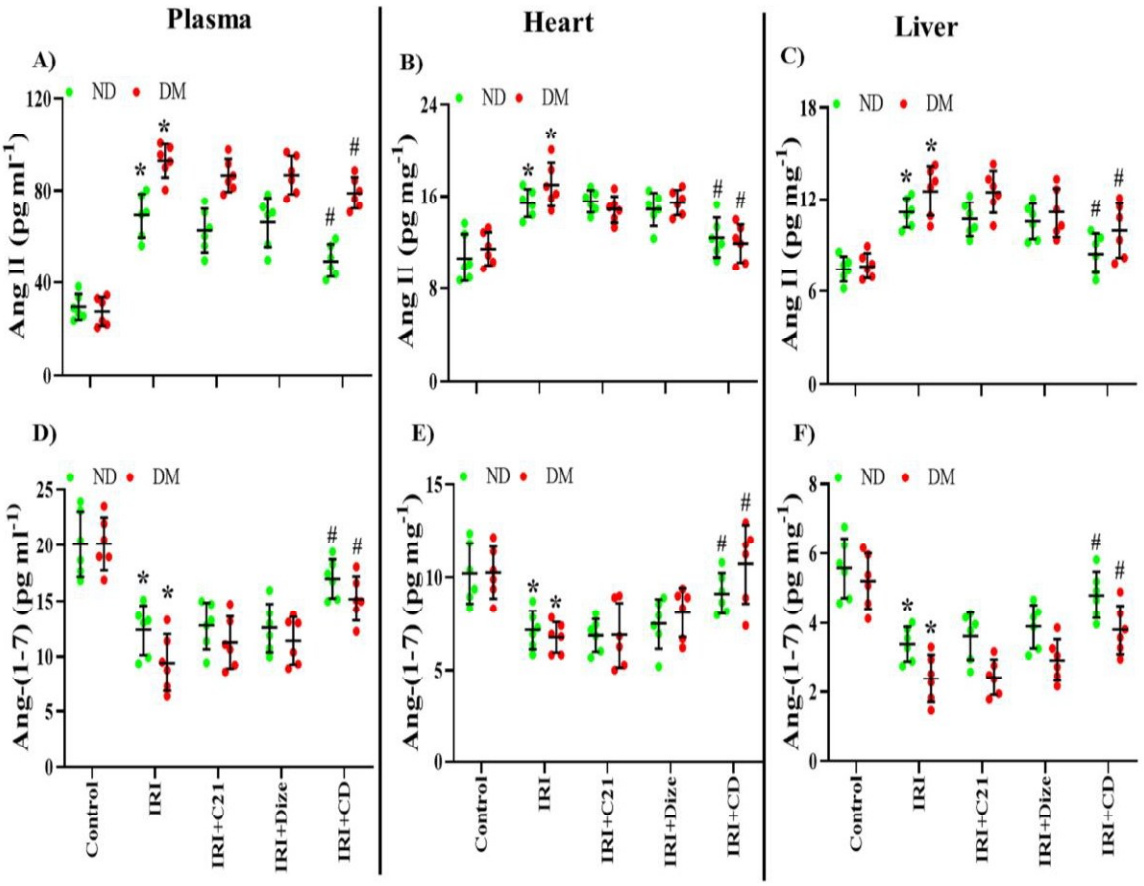

Figure 5.33 Effect of AT2R and ACE2 activation on protein levels of Ang II, Ang (1-7) in plasma, heart, and liver tissues.

A-F: Protein expression of Ang II and Ang (1-7) in plasma (A, D), heart (B, E) and liver (C, F) were assessed by ELISA (n=6). Data are represented as mean ± S.D. from three independent experiments. Two-way ANOVA with Tukey's multiple comparison test was utilized for statistical comparison. (*) $p < 0.05$ vs Control; (#) $p < 0.05$ vs IRI.

Urinary AGT was significantly higher ($P < 0.05$) in DM-IRI rats compared to ND-IRI rats. The C21 and Dize combination therapy have significantly reduced ($P < 0.05$) the urinary AGT levels as compared to ND/DM-IRI rats ***(Figure 5.32 G)***. Likewise, plasma, cardiac,

and hepatic Ang II levels were found to be markedly increased ($P < 0.05$) after IRI in ND and DM rats as compared to respective controls ***(Figure 5.33 A-C)***. Except for systemic circulation, the cardiac and hepatic Ang II levels were found to be higher in DM-IRI rats in comparison to ND-IRI rats. Further, C21 and Dize combination therapy have effectively reduced Ang II levels compared to ND/DM-IRI rats ***(Figure 5.33 A-C)***. Further, we also determine the Ang (1-7) levels in the systemic circulation, cardiac, and hepatic tissue. We found that the Ang (1-7) levels were significantly reduced ($P < 0.05$) by IRI as compared to ND and DM rats ***(Figure 5.33 D-F)***. Interestingly, DM-IRI rats showed a marked reduction in Ang (1-7) levels as compared to ND-IRI rats. Further, combination treatment has significantly improved ($P < 0.05$) the Ang (1-7) levels in plasma, cardiac and hepatic tissue as compared to ND/DM-IRI rats ***(Figure 5.33 D-F)***. None of the monotherapy has altered the Ang II and Ang (1-7) levels across the groups ***(Figure 5.33 A-F)***.